Representing plants as rigid cylinders in experiments and models

Vargas Luna, A; Crosato, A; Calvani, G; Uijttewaal, WSJ

DOI
10.1016/j.advwatres.2015.10.004

Publication date
2016

Document Version
Accepted author manuscript

Published in
Advances in Water Resources

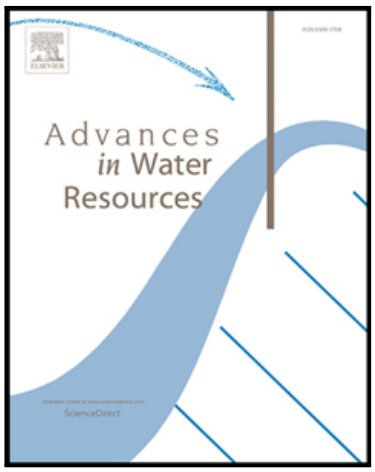

Representing plants as rigid cylinders in experiments and models

Andrés Vargas-Luna , Alessandra Crosato , Giulio Calvani , WimS.J. Uijttewaal

PII: S0309-1708(15)00241-9
DOI: 10.1016/j.advwatres.2015.10.004
Reference: ADWR 2486

To appear in: *Advances in Water Resources*

Received date: 29 January 2015
Revised date: 24 August 2015
Accepted date: 9 October 2015

Please cite this article as: Andrés Vargas-Luna , Alessandra Crosato , Giulio Calvani , WimS.J. Uijttewaal , Representing plants as rigid cylinders in experiments and models, *Advances in Water Resources* (2015), doi: 10.1016/j.advwatres.2015.10.004

Highlights

- We explore the correspondence between real plants and their rigid-cylinder description
- Experiments, numerical models and real rivers are combined in the analyses
- The cylinders diameter is relevant in representing the effects of the tested plants
- Numerical models can represent the effects of high-density vegetation

Representing plants as rigid cylinders in experiments and models

Andrés Vargas-Luna[a, b, *], Alessandra Crosato[a, c], Giulio Calvani[a,d], Wim S.J. Uijttewaal[a]

[a] Faculty of Civil Engineering and Geosciences, Delft University of Technology, PO Box 5048, 2600 GA Delft, The Netherlands

[b] Pontificia Universidad Javeriana, Cra. 7 No. 40-62, Bogotá D.C., Colombia

[c] Department of Water Engineering, UNESCO-IHE, PO Box 3015, 2601 DA Delft, The Netherlands

[d] Department of Civil and Environmental Engineering, University of Florence, P.zza S.Marco, 4 - 50121 Florence, Italy

* Corresponding author: Andrés Vargas-Luna,
Assistant professor, Pontificia Universidad Javeriana. PhD candidate, Delft University of Technology.
E-mail addresses: A.Vargasluna@tudelft.nl ; avargasl@javeriana.edu.co (Andrés Vargas-Luna)
Postal address: PO Box 5048, 2600 GA Delft. Tel.: +31(0)152785974.

ABSTRACT:

Simulating the morphological adaptation of water systems often requires including the effects of plants on water and sediment dynamics. Physical and numerical models need representing vegetation in a schematic easily-quantifiable way despite the variety of sizes, shapes and flexibility of real plants. Common approaches represent plants as rigid cylinders, but the ability of these schematizations to reproduce the effects of vegetation on morphodynamic processes has never been analysed systematically. This work focuses on the consequences of representing plants as rigid cylinders in laboratory tests and numerical simulations. New experiments show that the flow resistance decreases for increasing element Reynolds numbers for both plants and rigid cylinders. Cylinders on river banks can qualitatively reproduce vegetation effects on channel width and bank-related processes. A comparative review of numerical simulations shows that Baptist's method that sums the contribution of bed shear stress and vegetation drag, underestimates bed erosion within sparse vegetation in real rivers and overestimates the mean flow velocity in laboratory experiments. This is due to assuming uniform flow among plants and to an overestimation of the role of the submergence ratio.

Keywords: vegetation, rigid cylinders, morphodynamics, laboratory experiments, numerical modeling

1 INTRODUCTION

There is increasing awareness of the need to include the effects of vegetation in studies dealing with the morphological response of rivers and estuaries (e.g., [1, 2]). Numerical models and laboratory experiments (e.g., [3]) have recently shown that riparian vegetation can reduce river braiding and vegetation growth on point bars has been recognized as one of the major factors governing river meandering (e.g. [4-7]).

Plants increase the local hydraulic roughness, reducing flow velocity and bed-shear stress (e.g., [8, 9]) and promoting sedimentation [10, 11]. Vegetation cover protects the soil, and root systems increase the soil strength against erosion. In the end, plants act as ecosystem engineers since they create the conditions that favour the survival and establishment of new vegetation [12-15]. The relevance of vegetation processes for the morphological response of rivers and estuaries has resulted in an increased amount of research from several disciplines based on field investigations, laboratory experiments, and numerical models (e.g., [16- 21]).

Considering the relevance of vegetation for flow resistance, much research focused on calculating the hydraulic roughness of vegetated beds (e.g., [24-26]), and on the drag imposed by arrays of cylinders under submerged [27, 28] and emergent conditions [29-31].

A number of mobile-bed laboratory experiments used alfalfa sprouts to analyse the morphological changes caused by the presence of vegetation [3, 32-34], the influence of riparian vegetation on bank erosion [35], and the morphological effects of its spatial distribution [36], among other aspects (e.g., [37, 38]). More recently, the use of alfalfa sprouts has been combined with the supply of wooden dowels in order to reproduce the combined effects of living vegetation and floating logs [39]. These works showed important aspects of the effects of vegetation on the morphology of river systems, but provided mere qualitative results due to the difficulty of translating the laboratory results to the real river scale (upscaling).

The study of the flow around isolated cylindrical elements started in the early 1950's (e.g., [40, 41]), but it was only twenty years later that arrays of cylinders were considered in laboratory experiments to

simulate vegetation (e.g., [42-44]). These studies helped identifying the relevance of the stems density and spatial distribution on flow resistance, flow field and sediment processes. Other studies showed that the representation of plants as rigid cylinders neglects the reconfiguration of plant foliage under flowing water [45, 46] which decreases the projected area and drag forces [47-51]. Several research contributions have advanced our understanding of how an array of cylinders modifies vertical velocity profiles [52-54] and turbulent structures [27, 55, 56], affecting bed load [57, 58] and suspended load [59, 60], as well as depositional processes [11, 61].

Rigid cylinders have been used in laboratory experiments also to analyse the flow-vegetation interaction in vegetated patches and on floodplains. Regarding vegetated floodplains, a considerable amount of experimental work has been carried out to study the effects of vegetation on overbank flow [62], shear-stresses at cross-sectional interfaces [63], hydraulic conveyance [64], stream-bank erosion [65], near-bank turbulence [66], turbulent coherent structures [67, 68], and flow field alterations [69]. A few studies have considered wake structures and flow field alterations on finite vegetation patches in channels with fixed beds [70-72] and even fewer studies have considered bed level changes around vegetation patches [73].

From the available modelling approaches that have been proposed to describe plants in a schematic easily-quantifiable way, the most common one represents vegetation as a set of rigid cylinders with given height, diameter, stem distribution and density (a review can be found in Vargas-Luna et al. [74]). However, linking the settings of rigid cylinders to real vegetation is an important unsolved issue. In nature it is possible to find plants that can be well represented by cylindrical rigid stems (Figure 1a), but in most cases it is simply impossible to represent the variability of their geometrical and physical characteristics by this basic approach (Figure 1b). Plant flexibility is considered only by a few models (e.g., [75]), but these models are not suitable for practical applications, which reinforces the common practice of using simpler approaches.

Figure 1.

Experiments with rigid cylinders have the advantage of using the approach adopted by a number of numerical models (e.g., [24, 25, 76, 77]). This allows using the numerical models to interpret the laboratory results for real systems, since upscaling is a known problem for all experiments dealing with vegetation and sediment. However, it is still unclear whether numerical models based on the rigid cylinder representation of vegetation provide realistic results at the scale of real rivers and estuaries.

This work explores the implications of representing plants as rigid cylinders by means of new laboratory experiments and by reviewing the results of published model simulations. The first set of experiments, carried out in a straight flume with glass walls (Flume No. 1), studies the correspondence between the effects of real and artificial vegetation and those of rigid cylinders on water flows. This aspect is addressed by comparing the hydraulic roughness of channel beds covered either with plants or with rigid cylinders under the same flow regimes. The second set of experiments analyses the evolution of a channel with erodible bed and banks (Flume No. 2) to explore the feasibility of using rigid cylinders to simulate the effects of floodplain vegetation on the channel width formation. A third set of experiments, carried out in a similar, but larger, flume (Flume No. 3), explores the feasibility of using rigid cylinders to simulate vegetated bank dynamics.

The work is complemented by a thorough review of the results obtained by two-dimensional (2D) morphodynamic models adopting Baptist's method to evaluate the consequences of using a rigid-cylinder schematization for the simulation of the morphological developments of real rivers. To substantiate the analysis of model results, the predictive capacity of the method developed by Baptist [25] in estimating water depth and mean flow velocity is assessed by comparing the results to the data obtained from the first set of experiments.

This paper represents a first step in assessing the effects of representing real vegetation with rigid cylinders in laboratory experiments and numerical models. The results allow identifying the limitations of the approach and provide some preliminary guidelines on its application.

2 THEORETICAL BACKGROUND: BAPTIST'S METHOD

The flow resistance estimator for vegetated beds considered in this study was developed by Baptist in 2005 [25]. It is based on a rigid-cylinder representation of vegetation and can be considered as representative of the models adopting this approach. Baptist's method predicts the total flow resistance of a river bed covered by vegetation, which forms the base for water depth predictions. Sediment transport and bed level changes predictions, instead, are derived by considering the bed shear stress, which is reduced by the presence of vegetation, resulting in more realistic bed level changes in the vegetated areas [78]. The method is implemented in the open-source Delft3D software (www.deltares.nl), computing the morphological changes of rivers, estuaries and coasts in two and three dimensions. This is the software used in the simulations reviewed in Section 5. Baptist's method performance was analysed and compared to the performance of a number of other models [74], where it proved to be one of the most complete vegetation models, since it is valid for both submerged and emergent plants, and the most accurate one with respect to predictions of laboratory data.

Baptist described plants as sets of rigid cylinders with a characteristic diameter, D, height, h_v, and stem surface density, m, defined as the number of stems, N, per bed surface area (Figure 2). The basic assumption is that vegetation has high density so that the vertical velocity profile of the flow within the plants can be assumed uniform and constant in vertical direction. It is important to note that the approach does not allow for combinations of different vegetation types, such as grass and trees, at the same location.

Figure 2.

Baptist derived an expression for the hydraulic resistance to a flow over (submerged) and through (emergent) vegetation from the momentum balance, based on the following assumption:

$$\rho g h S_w = \tau_b + \tau_v \quad (1)$$

where ρ is the mass density of water (kg/m^3); g is the acceleration due to gravity (m/s^2); h is the water depth (m); S_w is the longitudinal water surface slope (-); τ_b is the bed shear stress (N/m^2) and τ_v is the extra shear stress caused by vegetation (N/m^2).

According to Baptist, the bed shear stress, τ_b , in case of emergent vegetation (wet vegetation height is equal to water depth *h*), is given by

$$\tau_b = \frac{\rho g}{C_b^2} u_c^2 \tag{2}$$

and the extra shear stress exerted by the plants is expressed as

$$\tau_v = \frac{1}{2} \rho C_D a h u_c^2 \tag{3}$$

where C_b is the Chézy coefficient of the bare soil ($m^{1/2}/s$); C_D is the drag coefficient of the plants (-) (Baptist suggests using C_D = 1); *a* is the projected cylinders area per unit of volume (m^{-1}) [2]: $a = mD$ (*m* being the number of stems, *N*, per bed surface area in m^{-2} and *D* the reference cylinder diameter in m). Typical ranges for *a* for natural vegetation are 0.1 to 1.0 m^{-1} for open herbaceous and marsh types of vegetation [25], and 10 to 15 m^{-1} for natural grasslands. The depth averaged flow velocity through vegetation, u_c (m/s), is given by:

$$u_c = C_r \sqrt{h S_w} \tag{4}$$

Where C_r represents the total friction coefficient expressed in terms of Chézy coefficient ($m^{1/2}/s$), given by the expression

$$C_r = \sqrt{\frac{1}{1/C_b^2 + C_D a h / 2g}} \tag{5}$$

It is important to note that a larger value of the canopy density leads to a smaller value of C_r corresponding to a larger bed roughness.

For submerged vegetation, it is assumed that the water depth is much larger than the plant height and that the flow velocity is uniform between the plants, but has a logarithmic profile above them, starting from the value u_c, obtained by substituting the water depth *h* (m) with the plant height h_v (m) in Equation 3. The bed shear stress becomes

$$\tau_b = \frac{\rho g}{C_b'^2} u^2 \tag{6}$$

where $C_b^{'}$ represents the flow resistance of the bed between the plants in case of submerged vegetation, given by the expression

$$C_b^{'} = C_b + \frac{\sqrt{g}}{\kappa}\sqrt{1+\frac{C_D a h_v C_b^2}{2g}}\ln\left(\frac{h}{h_v}\right) \quad (7)$$

in which κ (=0.41) is the Von Kármán constant. It is important to note that Equation 7 results in a reduction of the bed shear stress with respect to bare soil and emergent vegetation, since $C_b^{'}$ is larger than C_b.

Considering the total water flow, including the flow between and above vegetation, the depth averaged flow velocity results

$$u = C_r^{'}\sqrt{hS_w} \quad (8)$$

in which $C_r^{'}$ is the total friction coefficient expressed in terms of the Chézy coefficient ($m^{1/2}/s$), given by:

$$C_r^{'} = \sqrt{\frac{1}{1/C_b^2 + C_D a h_v/2g}} + \frac{\sqrt{g}}{\kappa}\ln\left(\frac{h}{h_v}\right) \quad (9)$$

It is important to observe that higher canopy density *a*, and plant height h_v, result in a smaller value of $C_r^{'}$ and therefore larger bed roughness. The first term of Equation 9 is equivalent to C_r (Equation 5) with the water depth substituted by the plant height. The logarithmic term appears only for $h > h_v$ and in such case it increases the value of $C_r^{'}$, decreasing the average resistance, for larger submergence (water-depth to plant-height) ratios. The submergence ratio (h/h_v) has also shown to be of relevance for the study of turbulent structures (e.g., [79-81]) and longitudinal mixing processes [82, 83] in vegetated channels.

3 MATERIALS AND METHODS: LABORATORY EXPERIMENTS

3.1 Representation of vegetated flows using rigid cylinders

To assess the capability of representing the effects of real and artificial vegetation by using uniformly distributed arrays of rigid cylinders, we used the tilting glass-walled flume 14 m long and 0.40 m wide available at the Fluid mechanics Laboratory of Delft University of Technology (Fig. 3a). We compared the effects of four types of vegetation on hydraulic resistance considering several densities and plant heights.

To represent plants, we used rigid cylinders (wooden sticks with diameter, D, equal to 2×10^{-3} m and total height, H, equal to 0.20 m, Fig. 3b), two flexible artificial plants, composed by either plastic grass (Fig. 3c) or by leafy plastic plants (*Egeria densa*, Fig. 3d) and real plants belonging to the Piperaceae family (*Peperomia rotundifolia*, Fig. 3e). The plants were inserted in a 0.15 m layer of sand with median diameter, D_{50}, equal to 5×10^{-4} m and sorting index, $I = 0.5(D_{50}/ D_{16} + D_{84}/ D_{50})$, equal to 1.23 (Fig. 4) in staggered patterns (Fig. 2c). The characteristic diameter for the real and artificial plants was derived by dividing the frontal area of the plant by its height. Vegetation properties are summarized in Table 1.

Water and sediment were recirculated. Water level and bed surface profiles were measured with lasers located in a movable carriage above the flume. The mean water depth was calculated as the difference between the water level and bed surface profiles. The discharge was measured in the supply system with an ultrasonic flowmeter. Mean flow velocities were derived by dividing the discharge by the total cross-sectional area.

Figure 3.

Figure 4.

Table 1.

Bed slopes in the flume were set to 0.002 or 0.004 m/m, but these did not coincide with the slope of the water surface. The flow resistance in terms of the friction coefficient, C_f, of the vegetated bed was

obtained by using the one-dimensional steady flow momentum equation per unit width, valid for gradually varying flow:

$$u\frac{du}{dx}+g\frac{dz}{dx}+g\frac{dh}{dx}+\frac{C_f u^2}{R_h}=0 \qquad (10)$$

where z is the bed level elevation (m) in the longitudinal direction x (m), C_f is the friction coefficient (-), and R_h is the hydraulic radius (m), expressed as the cross-sectional area over the wetted perimeter. The friction coefficient can straightforwardly be linked to the Chézy coefficient by the expression $C_f = g/C_r^2$. As a glass-sided flume was used, sidewall corrections were applied by using the method proposed by Vanoni and Brooks [84].

The flow velocity in the experiments was imposed below the condition for sediment motion to avoid important hydrodynamic effects of excessive bed scouring and deposition. However, some additional trials were performed at the end of each test with higher flows to observe the influence of vegetation on sediment transport and bed development. The changes in bed surface were recorded by a video camera from the lateral glass wall at specific locations. The differences between the initial and final bed surface profiles extracted from the measurements were used to roughly analyse the erosion and deposition patterns.

3.2 Representation of the channel-width formation using rigid cylinders

Another set of experiments was carried out to qualitatively study the effects of rigid cylinders on floodplains on the main channel-width formation, the major question being whether rigid cylinders (wooden sticks) inserted in the banks of an excavated channel would decrease bank erosion as real vegetation in similar experimental tests (e.g., [34]). The tests were carried out in a 2.25 m long, 1.2 m wide and 0.20 m deep mobile-bed flume (Flume No. 2, see Figure 5) with fixed inlet and outlet. A pump placed in a tank beneath the flume outlet provided the flow discharge by recirculating the water to a basin located behind the inlet, where waves were dissipated by a set of vanes. The pump was connected to a power-regulated supply system enabling flow discharge variation. The flume was filled with sand having median diameter, D_{50}, equal to 9.5×10^{-4} m and sorting index, I, equal to 2.32 (Fig. 4).

A straight 0.09 m wide channel was excavated in the centre of the flume with an initial bed slope of 0.01 m/m. Vegetation was represented by arrays of toothpicks with diameter, D, of 2×10^{-3} m and a total height of 0.08 m, considering several combinations of patterns and densities (Fig. 5b). The toothpicks were inserted in the sand, leaving just 0.02 m above the surface (i.e. H_1 = 0.08, and penetration depth H_2 = 0.06 in Fig. 5c). The characteristics of the parallel and staggered vegetation arrays are listed in Table 2.

Figure 5.

Table 2.

Three discharge hydrographs, including constant and variable flows, having the same averaged value, were applied to each of the seven configurations described in Table 2. The hydrographs were selected on the basis of the intensive laboratory experiments performed by Byishimo [85] (Fig. 5d). The width changes with time were tracked by recording the evolution of the channel with a video camera located at the top of the flume with the help of a squared grid (0.05×0.05 m) placed above the flume. By analysing the central part of the channel at three locations far from the inlet and outlet, the average channel width was measured each 5 minutes from the recorded videos.

3.3 Representation of bank dynamics using rigid cylinders

A third laboratory setup, Flume No. 3, was used to analyse the effects of vegetation and flow variability on channel planform formation, see Fig. 6a. The mobile-bed flume was 5.0 m long, 1.2 m wide and 0.25 m deep. An initial 0.08 m wide channel was excavated in the centre of the flume, filled with the same sand used in Flume No 2 (Figure 4). The initial bed slope was 0.010 m/m. For this set of experiments a curved bend made from a PVC elbow was used as a geometrical perturbation at the inlet of the flume, see Fig. 6. This time, only the 0.20 m wide inlet was fixed, whereas the outlet was let free to allow lateral channel migration.

Figure 6.

The same type of wooden toothpicks of the previous setup was used, this time considering only parallel arrays, but including different heights, H_1, and penetration depths, H_2 (see Table 3 and Fig. 6b). The flow was regulated as in Flume No 2. The constant and variable discharges, having the same averaged value, are given in Fig. 6c. The planform changes in time were tracked by recording the evolution of the channel with a video camera.

Table 3.

4 RESULTS OF LABORATORY EXPERIMENTS

4.1 Representation of vegetated flows using rigid cylinders

Considering that the flow resistance of a vegetated bed depends on the combination of flow and vegetation properties, the results are presented as a function of the element Reynolds number, with the uniform diameter of plants as characteristic length, given as

$$\mathrm{Re}_D = \frac{uD}{\nu} \tag{11}$$

where ν is the cinematic viscosity of the fluid (m^2/s). The results are presented in Figure 7. The first observation is that for all vegetation types the flow resistance decreases as the element Reynolds number increases. The trend is more evident for real plants and plastic grass (Figs. 7a and 7b), as well as for low density plastic *Egeria Densa* (Fig. 7c), for which the points appear clearly aligned on a curve. Only for wooden sticks, the friction coefficient increases if the density increases (Fig. 7d). Analysing the figure, it is possible to observe that the friction coefficients obtained with wooden sticks (Fig. 7d) have the same order of magnitude as the ones obtained with real and plastic plants, with only a few exceptions. The wooden sticks, however, present the smallest element Reynolds numbers, which is due to their small diameter (2 mm). Other experiments found in the literature [31] show that rigid cylindrical rods with larger diameters have friction coefficients and element Reynolds numbers similar to those observed for real and artificial plants in our experiments, see Fig. 7d. As they offer more realistic results, it might be better to use rigid stems or wooden sticks with larger diameters (of about 8 mm). Experiments reported in [31] have comparable flow velocities (0.077-0.342 m/s) and

submergence ratios (1.3 – 2.0) with the experiments reported here. For *Egeria Densa*, the highest density results in more scattered points (Fig. 7c), whereas for the other vegetation types low and high densities result in similar friction coefficients (Figs. 7a and 7b).

The possible effects of foliage and flexibility can be analysed by comparing the results provided by the two types of plants with leaves: real vegetation and plastic *Egeria Densa*. Both plant types have similar leaf volumes, but the leaves of the real plants have lower stiffness than the plastic ones, see Figs. 3d and 3e. With 2,755 plants/m^2 (high density), the leaves of the more rigid *Egeria Densa* act as obstacles to the flow and result in higher roughness than the more flexible leaves of real plants (compare Fig. 7c and Fig. 7a). This means that for plants with foliage the flow resistance is not only affected by vegetation density (expressed as number of plants per unit area), but also by foliage and plant flexibility. Therefore, another definition of plant geometry and density should be adopted when describing foliated plants in order to include the effect of these properties on the flow resistance. Contrary to what previously found by other researchers (e.g. [79]), the submergence ratio, h/h_v, does not appear to affect the flow resistance coefficients in our experiments.

Figure 7.

About the additional trials with flow velocities higher than the conditions for sediment motion, bedforms formed downstream and upstream of the vegetation patch for all vegetation types and densities, with different erosional and depositional patterns. With low and medium density artificial grass (DG1 and DG2) local erosion and deposition patterns formed within the vegetation patch. In some cases the plants were completely covered by sediment in certain areas. High density grass (DG3) produced local erosion at the upstream end of the vegetation patch, but in this case much less sediment was deposited more downstream inside the vegetation patch. Erosion occurred at end of the flume. High density vegetation with leafs (real plants and artificial *Egeria Densa*) produced local erosion at the upstream end of the vegetated patch, but the sediment settled just downstream of the patch and not within vegetation. With low density, erosion and deposition patterns resembled those obtained with

low density grass. With wooden sticks, much less sediment was trapped within the elements. At the highest flow velocities local scour occurred around each rigid cylinder.

The results show the relevance of vegetation foliage and high density in general in reducing flow velocities within the plants, affecting sediment transport processes as well as erosional and depositional patterns.

4.2 Representation of channel-width formation using rigid cylinders

Figure 8 shows the channel-width evolution as a function of time for the three considered discharge conditions. As expected, most changes occurred in the first 20 minutes of the experiments. The equilibrium width as well as the time required to achieve it decreases as vegetation density increases. This figure also shows that the response in time of the channel-width and the equilibrium width reached at the end of each experiment are substantially different for each discharge regime. This behaviour shows that the frequency and magnitude of high and low flow sequences have a major impact on the channel formation. The response of the channel-width to the bank erosion pulses driven by the peak flows is more noticeable in the variable regime with less frequent but higher flow peaks (Hydrograph 2). In all cases, the bank erosion rates decrease with time until the equilibrium width is reached, which is clearly attributed to the decrease of water depth caused by channel widening.

Figure 8.

The values of the equilibrium width of the channels are shown in Figure 9. The experiments with vegetated banks lead to smaller widths compared to the cases without vegetation for the same flow conditions. Larger width reductions occurred with dense vegetation. Regarding the influence of the vegetation pattern, both the separation between elements (along the parallel and perpendicular direction of the flow) and the arrangement (staggered or parallel) were found relevant for the final channel width. Experiments with the same density and parallel pattern but different interchanged separation distances S_1 and S_2 in Fig. 5b (tests W-V3 and W-V4) showed similar behaviour for the variable discharge tests. However, a shorter interchanged separation of the elements in the perpendicular direction, S_2, reduces the initial bank erosion rates and the equilibrium widths with

constant discharge. According to our observations parallel configurations appear to be more effective on reducing bank erosion than the staggered ones, when comparing the equilibrium width obtained in experiments with the same density.

Figure 9.

4.3 Representation of bank dynamics using rigid cylinders

The tests allowed observing several typical processes of real rivers with vegetated floodplains: sinuosity formation, braiding index evolution, bank failure, scroll bar formation, and floating vegetation. Since no substantial difference between constant and variable discharge was found for the un-vegetated cases, the tests including vegetation were performed only under variable flow regimes. In general, narrower and more stable channels were obtained for the experiments with vegetated banks, as in the previous section. The planform evolution for the tests performed in this section is given as supplementary material.

Channel Sinuosity

Figure 10 shows the evolution of channel sinuosity as a function of time. Variations in sinuosity appear related to discharge variability and vegetation density. In the experiments without vegetation the overall sinuosity of the channel was relatively similar for constant (P-NV(C)) and variable discharges (P-NV), even if the bank erosion pulses driven by the high flows can be easily identified. In general, discharge variability provided a more stable channel. This can be attributed to channel incision during low flows. Comparing the results of tests shown in Figure 10, it is possible to observe that the sinuosity is lower with denser vegetation, demonstrating the effectiveness of the rigid cylinders in increasing the bank strength. Figure 10 shows also that a smaller penetration depth increases sinuosity significantly (compare P-V1 with P-V2 and P-V3, having the same vegetation density). Nevertheless, in the experiment P-V3 a significant reduction of the channel sinuosity was observed after the peak discharge at 240 minutes. This change in sinuosity occurred because the wooden sticks that were deposited on bars were suddenly transported downstream by the peak flow, reducing bank protection.

Figure 10.

Braiding degree

Figure 11 shows the planform obtained at the end of each experimental test. This figure shows the difference between the tests without vegetation (P-NV) and the tests with vegetation (P-V1 to P-V4). Un-vegetated channels eventually evolve in wide braided systems (Figs. 11b and 11c). Moreover, it is relevant to highlight the large difference among tests P-V1, P-V2, and P-V3 differing in penetration depth and vegetation length, see Table 3 and Figs. 11d, 11e, and 11f. A higher penetration depth results in a drastically more stable channel (Fig. 11d); larger plants with the same penetration depth (PV-2 and PV-3) result in larger eradication rates and a wider channel (compare Figs 11e and 11f).

Figure 11.

The results show that the reduction of the braiding degree in channels found in former laboratory experiments with the addition of real vegetation [3, 32-34] can be also obtained with rigid sticks.

Bank failure and large floating debris

Bank failure occurred due to toe erosion, as shown in Figure 12a. Subsequently, the material fallen in the channel acted as bank protection, retarding the next failure episode. This process has been identified also at the outer bends of real meandering rivers (e.g., [86]). Figure 12b shows how the eradicated sticks were later deposited on the bars more downstream, particularly at the bar edge, stabilizing and retaining sediment, deflecting the water flow and promoting erosion near the opposite bank, thus increasing channel sinuosity. Moreover, the sticks on bars increased channel stability in such a way that only one main channel was observed for a longer period, contrary to observations in tests with fixed vegetation or with un-vegetated banks. Assuming that the rigid elements used in these experiments have comparable relative size and properties to woody debris, it is possible to state that the observed processes resemble those occurring in real rivers in U.S.A. [87-89] and Europe (e.g., [90-93]). Results shown in Figure 12b also agree with the recent findings of the experimental work carried out by Betoldi et al. [39].

Scroll bars

The formation of scroll bars along the channel is recognizable due to sediment sorting. Figure 12c shows that fine sediment is deposited at the edge of a bar, whereas the coarser fraction settled more downstream as described in most meandering rivers (e.g., [94]).

Figure 12.

5 REPRESENTATION OF VEGETATED RIVERS PROCESSES ADOPTING BAPTIST'S METHOD

The performance of numerical models adopting Baptist's method is here assessed based on additional analysis based on our experimental findings and the comparative review of a number of published numerical tests. The numerical simulations were all carried out with similar, and therefore comparable, two-dimensional (2D) models developed from the open-source physics-based morphodynamic software Delft3D solving the Reynolds equations for incompressible fluid and shallow water.

The computations were carried out using a depth-averaged model provided with a parameterization of the 3D effects that become relevant for curved flow [95] and accounting for the effects of gravity on bed load direction [96, 97]. The effects of vegetation on bed roughness and sediment transport were accounted for according to Baptist's method, described in Section 2, computing the sediment transport rate as a function of τ_b (Equation 2 or 6) and the water depth as a function of the total bed shear stress, $\tau_b + \tau_v$ (Equations 1 to 9). Bed load was computed using Meyer-Peter and Müller's [98] sediment transport capacity formula. Suspended load was computed adopting the method developed by Galappatti and Vreugdenhil [99].

Delft3D computes the local bed level changes by means of sediment balance equations, resulting in temporal bed level changes in case of spatial imbalance of the sediment transport. Two different approaches are adopted: Exner's approach, valid for immediate adaptation of sediment transport to flow velocity, for bed load; and 2D advection-diffusion equations with sediment entrainment and

deposition appearing as forcing terms, for suspended load. Bank erosion is computed relating bank retreat to bed degradation at the toe of the bank [100].

The characteristics of all underlying mathematical equations and their numerical representation are described more in detail in the manuals, which can be downloaded from http://oss.deltares.nl/web/delft3d/manuals. The software can be downloaded from http://oss.deltares.nl/web/delft3d/source-code.

5.1 Reproduction of the effects of vegetation observed in experiments by Baptist's method

To study how well Baptist's method predicts the global flow resistance and mean flow velocity over vegetated beds we compared the values measured in the experiments carried out in Flume No 1 with model predictions. Measured Chézy coefficients were derived from the friction coefficients, C_f, by using the relation $C'_{r\,Measured} = \sqrt{g/C_f}$. Predictions for the wooden sticks were calculated with the properties of each tested array of cylinders. For the case of real and artificial plants, predictions were obtained by representative arrays of rigid cylinders with the vegetation height of each type of plant, but the characteristics of the highest-density wooden-stick configurations (see Section 4.1). The drag coefficient, C_D, was here assumed equal to unity and the Chézy coefficient for the bare soil, C_b, was obtained from the results of the experiments for the un-vegetated conditions.

The comparison between measured and estimated Chézy coefficients and mean flow velocities for the real and artificial plants, and rigid cylinders is shown in Figs 13 and 14, respectively. The most consistent predictions for the wooden sticks are obtained for the highest density configurations, which is in accordance with the assumptions of the method. The results show that Baptist's method leads to overestimation of Chézy coefficients and mean flow velocities, for real and artificial plants as well as for rigid cylinders, producing the underestimation of water depths. This is attributed here to: 1) the uncertainty in the value of the Chézy coefficient for the bare soil, which was here assigned on the basis of the un-vegetated cases, and 2) excessive reduction of global flow resistance as a function of the submergence ratio (see Equation 9), considering the small values of the Chézy coefficient that were derived for the experiments. A similar function of the submergence ratio appears also in equation

7, used for the computation of sediment transport in vegetated areas. Overestimation of the effects of the submergence ratio on the reduction of flow resistance explains both the reduction of morphological changes (Equation 7) and the overestimation of mean flow velocity (Equation 9). The term including the submergence ratio is related to a logarithmic velocity profile above vegetation, but corrections accounting for turbulence effects are not included. Baptist et al. [26] identified that the method performs better in cases with high values of the Chézy coefficient, but without providing explanations.

Figure 13

Figure 14

Figure 14 also shows that the estimated Chézy coefficients exhibit a noticeable variation only for the highest density configurations of rigid cylinders, whereas very similar values are obtained for each vegetation height in the other configurations. This behaviour results from the increase of the hydraulic roughness due to vegetation in Baptist's method which also depends on the magnitude of the Chézy coefficient for the bare soil, C_b. This can be seen if C_b is extracted from the squared root of the first term of equation 9, obtaining the expression

$$C_r^{'} = C_b \sqrt{\frac{1}{1+C_D a h_v C_b^2/2g}} + \frac{\sqrt{g}}{\kappa} \ln\left(\frac{h}{h_v}\right) \quad (12)$$

The first term of equation 12 shows that noticeable reductions of C_b are obtained with high values of $C_D a h_v C_b^2/2g$, which are not only reached with high densities, but also with relatively high values of C_b. However, values of C_b over 20 $m^{1/2}/s$ lead to similar estimations of this first term for a wide range of densities. This fact is especially important in mobile bed laboratory experiments in which low values of the Chézy coefficient for the bare soil are normally observed, pointing out relevant issues for upscaling processes as well.

5.2 Reproduction of the effects of floodplain vegetation on river morphology with Baptist's method

This part of the study reviews the numerical investigations performed by Baptist and de Jong [101] and by Crosato and Samir Saleh [20] on the Allier River upstream of Moulins, France. In the study area, the Allier is a highly-dynamic gravel-bed river at the transition between meandering and braided (e.g., [102]), forming large meanders with side channels and central bars. Floodplain vegetation is characterized by pioneer species and grass on the lowest and highest parts of point bars, as well as by softwood forest in the highest and oldest parts of the floodplains. The simulations of Baptist and de Jong [101] regarded the prediction of the morphological changes during one year characterized by a major flood event. Crosato and Samir Saleh [20] simulated the effects of floodplain vegetation on the river planform formation. The model by Crosato and Samir Saleh was set up to represent a river having the characteristics of the Allier near Moulins, starting from a straight channel. Several cases were analysed, including bare floodplains and floodplains uniformly covered by either pioneer vegetation or grass, with constant or variable discharge. For variable discharge and vegetated floodplains, the sediment deposits that became dry during low-flows were colonized by plants having the same characteristics as floodplain vegetation (either pioneer vegetation or grass). The sediment was assumed uniform with particle diameter equal to 5×10^{-3} m with the same characteristics in the entire model domain, including channel and floodplains.

Both studies adopted a Chézy value of 50 $m^{1/2}/s$ to represent bare-bed roughness and considered only bed load transport. Coherently with the rigid-cylinder representation, assuming turbulent flow [25], both studies imposed $C_D = 1$ for all vegetation types. The values used for plant height, h_v, stem diameter, D, and density, m, are listed in Table 4.

Table 4.

By comparing model results to measurements, Baptist and de Jong [101] show the importance of including floodplain vegetation to simulate the effects of floods on the Allier River morphology. Their model generally underestimated the morphological changes in both cases, with and without floodplain vegetation. In particular, the model under predicted the erosion rates and did not simulate the observed sedimentation in the higher floodplain parts covered by forest (trees), as well as the filling of the

oxbow lake. Without vegetation, the model strongly under predicted bed erosion in the main channel bed, but led to more realistic bed erosion in the floodplain area.

Considering that in the study area sediment varies from sand to coarse gravel, the under prediction of the morphological changes can be partly attributed to not accounting for sediment grading. Finer sediment is more mobile: it is more easily eroded and more easily transported to the upper parts of the floodplains. Accounting for sand could have allowed simulating the filling up of the oxbow lake and the sedimentation in the higher parts of the floodplains. Moreover, the model did not include bank erosion, which was one of the major causes of erosion.

As bed erosion within trees is not reproduced by the model with floodplain vegetation, but is observable in the model without vegetation, we can conclude that the problem is due to the representation of vegetated flows in the model. Moreover, the water flow within trees is not uniform and presents accelerations and decelerations leading to bed erosion and sedimentation, respectively. Assuming uniform flow between the plants is therefore a clear shortcoming of the model in case of sparse vegetation, with the result of neglecting important morphological changes.

Starting from a straight channel having the characteristics of the Allier River, Crosato and Samir Saleh [20] obtained a strongly braided channel without floodplain vegetation, a channel with drastically lower braiding intensity with low-density pioneer vegetation, and a channel at incipient meandering conditions with low-density grass on floodplains.

A number of laboratory experiments show similar results (e.g., [3]), whereas similar effects of vegetation are observable also in real rivers (e.g., [103]). However, it seems not realistic to assume that pioneer vegetation with the very low density of 4.5 elements per square meter has such a strong effect on real rivers. The results therefore indicate that the vegetation model most probably over predicts the stabilizing effects of low-density vegetation, which can be due to overprediction of bed roughness reduction within the plants, as presented in Section 5.1.

5.3 Reproduction of sedimentation rates on vegetated floodplains with Baptist's method

This part of the study reviews the results of the investigations carried out by Facchini [104], Facchini et al. [105] and Montes Arboleda et al. [106] to investigate the capability of the model in representing the effects of floodplain vegetation on local sedimentation rates.

Facchini [104] and Facchini et al. [105] simulated the short-term sedimentation rates on the Ewijkse Plaat, a floodplain of the Waal River, near Nijmegen, the Netherlands for the period 1990-1997 for which measured bed topographies, erosion and sedimentation maps and averaged sedimentation rates in the study areas as well as the temporal evolution of vegetation were available [107, 108]. The model used daily measured discharges and included both bed load and suspended load. Three sediment fractions were considered: coarse sand, medium sand and silt. Sediment inputs were derived by Asselman [109]. Vegetation was represented as in Table 4.

Montes Arboleda et al. [106] simulated the floodplain sedimentation rates along the Waal River on the long term and compared the model results with the average sedimentation rates derived from the analysis of coring data carried out by Middelkoop [110]. The study site is the floodplain of the Waal River between the cities of Nijmegen and Tiel including the Ewijkse Plaat. The major difference between the two studies lies in the time period, since Montes et al. studied the river in 1800 A.D.

The daily discharges were derived from the water levels measured at Arnhem and the discharges measured at Cologne using the Q-h relationships derived by van Vuuren [111]. Montes at al. considered two sediment types: sand and silt. Assuming that the incoming sediment concentrations were the same as at present, the same rating curve developed by Asselman [109] was used as upstream boundary condition. Vegetation data were derived from the ecotope maps reconstructed by Maas et al. [112], showing that also at that time the dominant floodplain vegetation was herbaceous or grass. Three vegetation types were considered: natural grass, reed and softwood forest (Table 4).

The results of Facchini [106] show that the model reproduces the averaged short-term bed level rises quite well (period 1994-1995: computed 0.081 m, measured 0.080 m; period 1994-1997: computed 0.101 m, measured 0.090 m) .

The results of Montes Arboleda et al. [106] show that the model reproduces well also the long-term floodplain sedimentation rates. The averaged historical sedimentation rates derived from coring of the floodplain soil for the period around 1800 AD ranges between 5 and 16 mm/year, whereas the computed sedimentation rates ranged between 6.3 and 13.5 mm/year. Moreover, the results show that vegetation results in higher sedimentation rates in the areas close to the main river channel and lower sedimentation rates in the farther areas of the floodplain, confirming the observations by Pizzuto [113]. The increased flow resistance exerted by vegetation leads to flow concentration in the main channel and reduces flow velocity, as well as suspended solids concentration over the floodplains, as reported also by Villada Arroyave and Crosato [21]. Even though flow velocity reduction enhances sediment deposition, the reduction of sediment concentration over the floodplain results in lower sedimentation rates, especially in the areas that are far from the channel.

6 CONCLUSIONS

In this paper we have managed to combine experimental work from three experimental settings, ranging from flow interaction with vegetation to vegetation induced bank migration. The first laboratory setup shows that the hydraulic roughness of vegetated beds decreases for increasing element Reynolds numbers, which is according to expectations. Rigid cylinders show the same trends and have friction coefficients of the same order of magnitude, but are characterized by element Reynolds numbers which are significantly smaller than the ones of real and plastic plants. Diameters of 8.3 mm used by Cheng [31] offer the best resemblance with the results of our real and plastic plants. Plant flexibility was detected to be relevant for the flow resistance particularly for plants with foliage. Surprisingly, the submergence ratio (h/h_v) was not found to affect the flow resistance in our laboratory experiments.

Laboratory setups two and three allowed establishing the applicability of rigid cylinders to qualitatively represent the morphodynamic processes of channels with vegetated floodplains. Results obtained in Flume No. 2 showed the potential of using rigid cylinders to study the influence of vegetation on the channel-width formation. Parallel configurations of rigid cylinders were found more

effective in reducing the channel-width than staggered configurations. The results of the experiments carried out in Flume No. 3 show that it is possible to qualitatively reproduce bank dynamics-related processes and reduce the river braiding degree by placing rigid cylinders on the floodplains. The height of the rigid cylinders above the bed and the penetration depth into the bed were found of relevance for the channel planform formation.

Numerical models adopting Baptist's method to reproduce the effects of plants provide satisfactory results for high-density grass and herbaceous vegetation. Particularly satisfactory are the predictions of sedimentation rates on vegetated floodplains. The method performed well also for the reproduction of the effects of floodplain vegetation on the river planform formation, although the results are only qualitative. However, in general Baptist's method leads to overestimation of the bed protection effects of low-density vegetation, in particular for trees and pioneer plants. This overestimation is mainly due to the basic assumption that the flow velocity is uniform among the plants, which is not true for low-density vegetation. In some cases, trees are found to enhance rather than prevent bed erosion, since they act as isolated roughness elements (e.g., [114]). Therefore Baptist's method does not appear suitable to reproduce the effects of trees and isolated plants as well as patchy vegetation distributions (e.g., [115]).

Representation of the effects of vegetation in the model is based on three parameters: the canopy density, a, the plant height, h_v, and the drag coefficient, C_D. These parameters are multiplied to each-other to form a bulk parameter weighing the effects of plants on the bed shear stress in Equations 5, 7 and 9. The plant height appears again in the submergence ratio in Equations 7 and 9, in which higher values of the ratio result in smoother channels beds.

Comparison between data measured in the laboratory and predictions show that Baptist's method overpredicts mean flow velocities, underpredicting water depths. This can be attributed to an excessive reduction of global flow resistance related to the submergence ratio of vegetation, especially for low Chézy coefficients (rough beds). This leads also to overestimations of the effects of submerged vegetation in reducing local morphological changes (erosion and deposition).

Baptist [7] assigns a value between 1 and 2 to the drag coefficient, whereas a number of researchers (e.g., [116-118]) suggest using C_D = 1 for multiple cylinders and high Reynolds numbers (turbulent flows). We argue that a coherent representation of plants as rigid cylinders requires adopting always the same value for the drag coefficient, this being the value derived for cylinders. We therefore suggest imposing C_D equal to unity in numerical models. In this case, vegetation is basically distinguished by canopy density, a, and plant height, h_v. This simpler characterization would allow for a clearer interpretation of the morphodynamic effects of different types of vegetation.

Acknowledgements

We thank Andrea D'Alpaos and two anonymous reviewers for their comments on the manuscript. Special thanks go to P.X. Salgado and P. Byishimo for the valuable assistance in the laboratory experiments. Thanks also to May Samir Saleh for making her data available for the study. Andrés Vargas-Luna is grateful to COLCIENCIAS (Colombian Administrative Department of Science, Technology and Innovation), and to Pontificia Universidad Javeriana, the institutions that support financially his studies in the Netherlands.

Supplementary material

A. Planform evolution for the tests performed in Flume No. 3.

Notation:

a	=	Projected plant area per unit volume (m^{-1}), = mD
B	=	Channel width (m)
B_e	=	Equilibrium channel width (m)
C	=	Chézy coefficient obtained from the measurements ($m^{1/2}/s$)
C_f	=	Friction coefficient obtained from the measurements (-), = g/C^2
C_b	=	Chézy coefficient of the bare soil for vegetated beds ($m^{1/2}/s$)
$C_b^{'}$	=	Chézy coefficient of the bed for submerged plants ($m^{1/2}/s$)
C_D	=	Mean drag coefficient of the vegetation (-)
C_r	=	Chézy coefficient for the global resistance of emergent plants ($m^{1/2}/s$)
$C_r^{'}$	=	Chézy coefficient for the global resistance of submerged plants ($m^{1/2}/s$)
D	=	Plants characteristic diameter (m)
g	=	gravity acceleration (m/s^2)
h	=	Water depth (m)
h_v	=	Vegetation height (m)
I	=	Sorting index (-)
I_S	=	Channel sinuosity (-)
m	=	Stems surface density (m^{-2})
Q	=	Flow discharge (m^3/s)
R_h	=	Hydraulic radius (m)
Re_D	=	Element Reynolds number (-)
s_1	=	Separation between elements in parallel direction to the flow (m)
s_2	=	Separation between elements in perpendicular direction to the flow (m)
$u(z)$	=	Vertical velocity profile (m/s)
u	=	Mean flow velocity (m/s)
u_c	=	Mean flow velocity in the vegetation layer (m/s)
S_w	=	Longitudinal water surface slope (-)
ν	=	Cinematic viscosity of the fluid (m^2/s)
ρ	=	Mass density of water (kg/m^3)
κ	=	Von Kármán's constant (-), = 0.41
τ_b	=	Bed shear stress (N/m^2)
τ_v	=	Shear stress caused by vegetation (N/m^2)

References

[1] E. J. Hickin, Vegetation and river channel dynamics, Canadian Geographer / Le Géographe canadien 28 (2) (1984) 111-126. http://dx.doi.org/10.1111/j.1541-0064.1984.tb00779.x

[2] H. M. Nepf, Flow and transport in regions with aquatic vegetation, Annual Review of Fluid Mechanics 44 (1) (2012) 123-142. http://dx.doi.org/10.1146/annurev-fluid-120710-101048.

[3] M. Tal, C. Paola, Dynamic single-thread channels maintained by the interaction of flow and vegetation, Geology 35 (4) (2007) 347-350. http://dx.doi.org/10.1130/G23260A.1

[4] G. Parker, Y. Shimizu, G. V. Wilkerson, E. C. Eke, J. D. Abad, J. W. Lauer, C. Paola, W. E. Dietrich, V. R. Voller, A new framework for modeling the migration of meandering rivers, Earth Surface Processes and Landforms 36 (1) (2011) 70-86. http://dx.doi.org/10.1002/esp.2113

[5] K. Asahi, Y. Shimizu, J. Nelson, G. Parker, Numerical simulation of river meandering with self-evolving banks, Journal of Geophysical Research: Earth Surface 118 (2013) 1-22. http://dx.doi.org/10.1002/jgrf.20150

[6] E. Eke, G. Parker, Y. Shimizu, Numerical modeling of erosional and depositional bank processes in migrating river bends with self-formed width: Morphodynamics of bar push and bank pull, Journal of Geophysical Research: Earth Surface 119 (7) (2014) 1455-1483. http://dx.doi.org/10.1002/2013JF003020.410

[7] W. Bertoldi, A. Siviglia, S. Tettamanti, M. Tofolon, D. Vetsch, S. Francalanci, Modeling vegetation controls on fluvial morphological trajectories, Geophysical Research Letters (2014) http://dx.doi.org/10.1002/2014GL061666

[8] T. Tsujimoto, Fluvial processes in streams with vegetation, Journal of Hydraulic Research 37 (6) (1999) 789-803. http://dx.doi.org/10.1080/00221689909498512

[9] S. J. Bennett, T. Pirim, B. D. Barkdoll, Using simulated emergent vegetation to alter stream flow direction within a straight experimental channel, Geomorphology 44 (1-2) (2002) 115-126. http://dx.doi.org/10.1016/S0169-555X(01)00148-9.3

[10] W. Wu, Z. He, Effects of vegetation on flow conveyance and sediment transport capacity, International Journal of Sediment Research 24 (3) (2009) 247-259. http://dx.doi.org/10.1016/S1001-6279(10)60001-7

[11] L. Zong, H. Nepf, Spatial distribution of deposition within a patch of vegetation, Water Resources Research 47 (2011) W03516, http://dx.doi.org/10.1029/2010WR009516

[12] W. Bertoldi, N. A. Drake, A. M. Gurnell, Interactions between river flows and colonizing vegetation on a braided river: exploring spatial and temporal dynamics in riparian vegetation cover using satellite data, Earth Surface Processes and Landforms 36 (11) (2011) 1474-1486. http://dx.doi.org/10.1002/esp.2166

[13] A. M. Gurnell, Plants as river system engineers, Earth Surface Processes and Landforms 39 (2014) 4-25. http://dx.doi.org/10.1002/esp.3397.

[14] A. M. Gurnell, A. J. Boitsidis, K. Thompson, N. J. Clifford, Seed bank, seed dispersal and vegetation cover: Colonization along a newly-created river channel, Journal of Vegetation Science 17 (5) (2006) 665-674. http://dx.doi.org/10.1111/j.1654-1103.2006.tb02490.x

[15] A. M. Gurnell, W. Bertoldi, D. Corenblit, Changing river channels: The roles of hydrological processes, plants and pioneer fluvial landforms in humid temperate, mixed load, gravel bed rivers, Earth-Science Reviews 111 (1-2) (2012) 129-141. http://dx.doi.org/10.1016/j.earscirev.2011.11.005

[16] A. B. Murray, C. Paola, Modelling the effect of vegetation on channel pattern in bedload rivers, Earth Surface Processes and Landforms 28 (2) (2003) 131-143. http://dx.doi.org/10.1002/esp.428

[17] C. Camporeale, L. Ridolfi, Convective nature of the planimetric instability in meandering river dynamics, Physical Review E 73 (2) (2006) 026311. http://dx.doi.org/10.1103/PhysRevE.73.026311

[18] E. Perucca, C. Camporeale, L. Ridolfi, Significance of the riparian vegetation dynamics on meandering river morphodynamics, Water Resources Research 43 (2007) W03430, http://dx.doi.org/10.1029/2006WR005234

[19] P. Perona, C. Camporeale, E. Perucca, M. Savina, P. Molnar, P. Burlando, L. Ridolfi, Modelling river and riparian vegetation interactions and related importance for sustainable ecosystem management, Aquatic Sciences 71 (3) (2009) 266-278. http://dx.doi.org/10.1007/s00027-009-9215-1

[20] A. Crosato, M. Samir Saleh, Numerical study on the effects of floodplain vegetation on river planform style, Earth Surface Processes and Landforms 36 (6) (2011) 711-720. http://dx.doi.org/10.1002/esp.2088

[21] J. Villada Arroyave, A. Crosato, Effects of river floodplain lowering and vegetation cover, Proceedings of the ICE - Water Management 163 (9) (2010) 457-467. http://dx.doi.org/10.1680/wama.900023

[22] C. Camporeale, E. Perucca, L. Ridolfi, A. M. Gurnell, Modeling the interactions between river morphodynamics and riparian vegetation, Reviews of Geophysics (2013) http://dx.doi.org/10.1002/rog.20014

[23] L. Solari, M. Van Oorschot, B. Belletti, D. Hendriks, M. Rinaldi, A. Vargas-Luna, Advances on modelling riparian vegetation-hydromorphology interactions, River Research and Applications (2015) *In press*. http://dx.doi.org/10.1002/rra.2910

[24] B. M. Stone, H. T. Shen, Hydraulic resistance of flow in channels with cylindrical roughness, Journal of Hydraulic Engineering 128 (5) (2002) 500-506. http://dx.doi.org/10.1061/(ASCE)0733-9429(2002)128:5(500)

[25] M. J. Baptist, Modelling floodplain biogeomorphology, Ph.D. thesis, Delft University of Technology, ISBN 90-407-2582-9 (2005).

[26] M. J. Baptist, V. Babovic, J. Rodríguez Uthurburu, M. Keijzer, R. Uittenbogaard, A. Mynett, A. Verwey, On inducing equations for vegetation resistance, Journal of Hydraulic Research 45 (4) (2007) 435-450. http://dx.doi.org/10.1080/00221686.2007.9521778

[27] H. M. Nepf, Drag, turbulence, and diffusion in flow through emergent vegetation, Water Resources Research 35 (2) (1999) 479489, http://dx.doi.org/10.1029/1998WR900069

[28] H. Tang, Z. Tian, J. Yan, S. Yuan, Determining drag coefficients and their application in modelling of turbulent flow with submerged vegetation, Advances in Water Resources 69 (2014) 134-145. http://dx.doi.org/10.1016/j.advwatres.2014.04.006

[29] Y. Tanino, H. Nepf, Laboratory investigation of mean drag in a random array of rigid, emergent cylinders, Journal of Hydraulic Engineering 134 (1) (2008) 34-41. http://dx.doi.org/10.1061/(ASCE)0733-9429(2008)134:1(34)

[30] U. C. Kothyari, K. Hayashi, H. Hashimoto, Drag coefficient of unsubmerged rigid vegetation stems in open channel flows, Journal of Hydraulic Research 47 (6) (2009) 691-699. http://dx.doi.org/10.3826/jhr.2009.3283

[31] N. S. Cheng, Representative roughness height of submerged vegetation, Water Resources Research 47 (8) (2011) W08517. http://dx.doi.org/10.1029/2011WR010590

[32] K. Gran, C. Paola, Riparian vegetation controls on braided stream dynamics, Water Resources Research 37 (12) (2001) 3275-3283, http://dx.doi.org/10.1029/2000WR000203

[33] C. A. Braudrick, W. E. Dietrich, G. T. Leverich, L. S. Sklar, Experimental evidence for the conditions necessary to sustain meandering in coarse-bedded rivers, Proceedings of the National Academy of Sciences 106 (40) (2009) 16936-16941. http://dx.doi.org/10.1073/pnas.0909417106

[34] M. Tal, C. Paola, Effects of vegetation on channel morphodynamics: results and insights from laboratory experiments, Earth Surface Processes and Landforms 35 (9) (2010) 1014-1028. http://dx.doi.org/10.1002/esp.1908

[35] C. Jang, Y. Shimizu, Vegetation effects on the morphological behavior of alluvial channels, Journal of Hydraulic Research 45 (6) (2007) 763-772. http://dx.doi.org/10.1080/00221686.2007.9521814

[36] W. M. van Dijk, R. Teske, W. I. van de Lageweg, M. G. Kleinhans, Effects of vegetation distribution on experimental river channel dynamics, Water Resources Research 49 (11) (2013) 7558-7574. http://dx.doi.org/10.1002/2013WR013574

[37] C. Paola, K. Straub, D. Mohrig, L. Reinhardt, The "unreasonable effectiveness" of stratigraphic and geomorphic experiments, Earth-Science Reviews 97 (1-4) (2009) 1-43. http://dx.doi.org/10.1016/j.earscirev.2009.05.003

[38] M. G. Kleinhans, W. M. van Dijk, W. I. van de Lageweg, D. C. Hoyal, H. Markies, M. van Maarseveen, C. Roosendaal, W. van Weesep, D. van Breemen, R. Hoendervoogt, N. Cheshier, Quantifiable effectiveness of experimental scaling of river- and delta morphodynamics and stratigraphy, Earth-Science Reviews 133 (0) (2014) 43-61, http://dx.doi.org/10.1016/j.earscirev.2014.03.001

[39] W. Bertoldi, M. Welber, A. Gurnell, L. Mao, F. Comiti, M. Tal, Physical modelling of the combined effect of vegetation and wood on river morphology, Geomorphology 246 (2015) 178-187, http://dx.doi.org/10.1016/j.geomorph.2015.05.038

[40] R. K. Finn, Determination of the drag on a cylinder at low Reynolds numbers, Journal of Applied Physics 24 (6) (1953) 771-773. http://dx.doi.org/10.1063/1.1721373

[41] D. J. Tritton, Experiments on the flow past a circular cylinder at low Reynolds numbers, Journal of Fluid Mechanics 6 (1959) 547-567. http://dx.doi.org/10.1017/S0022112059000829

[42] R. Li, H. Shen, Effect of tall vegetations on flow and sediment, Journal of the Hydraulics Division, ASCE 99 (5) (1973) 793-813.

[43] S. Petryk, G. Bosmajian, Analysis of flow through vegetation, Journal of the Hydraulics Division 101 (7) (1975) 871-884.

[44] E. W. Tollner, B. J. Barfield, C. Vachirakomwatana, C. T. Haan, Sediment deposition patterns in simulated grass filters, Transactions, American Society of Agricultural Engineers 20 (5) (1977) 940-944.

[45] B. Statzner, N. Lamouroux, V. Nikora, P. Sagnes, The debate about drag and reconfiguration of freshwater macrophytes: comparing results obtained by three recently discussed approaches, Freshwater Biology 51 (11) (2006) 2173-2183. http://dx.doi.org/10.1111/j.1365-2427.2006.01636.x

[46] J. Aberle, J. Järvelä, Flow resistance of emergent rigid and flexible floodplain vegetation, Journal of Hydraulic Research 51 (1) (2013) 33-45. http://dx.doi.org/10.1080/00221686.2012.754795

[47] F. Gosselin, E. de Langre, B. A. Machado-Almeida, Drag reduction of flexible plates by reconfiguration, Journal of Fluid Mechanics 650 (2010) 319-341. http://dx.doi.org/10.1017/S0022112009993673

[48] E. de Langre, A. Gutierrez, J. Coss, On the scaling of drag reduction by reconfiguration in plants, Comptes Rendus Mcanique 340 (1-2) (2012) 35-40, biomimetic flow control. http://dx.doi.org/10.1016/j.crme.2011.11.005

[49] A. Dittrich, J. Aberle, T. Schoneboom, Environmental Fluid Mechanics: Memorial colloquium on environmental fluid mechanics in honour of Prof. Gerhard H. Jirka, IAHR Monographs, CRC Press, 2012, Ch. Drag forces and flow resistance of flexible riparian vegetation, 195-215. http://dx.doi.org/10.1201/b12283-11

[50] F. Siniscalchi, V. Nikora, Dynamic reconfiguration of aquatic plants and its interrelations with upstream turbulence and drag forces, Journal of Hydraulic Research 51 (1) (2013) 46-55. http://dx.doi.org/10.1080/00221686.2012.743486

[51] I. Albayrak, V. Nikora, O. Miler, M. T. O'Hare, Flow-plant interactions at leaf, stem and shoot scales: drag, turbulence, and biomechanics, Aquatic Sciences 76 (2) (2014) 269-294. http://dx.doi.org/10.1007/s00027-013-0335-2

[52] E. Kubrak, J. Kubrak, P. M. Rowiński, Vertical velocity distributions through and above submerged, flexible vegetation, Hydrological Sciences Journal 53 (4) (2008) 905-920. http://dx.doi.org/10.1623/hysj.53.4.905

[53] W. Huai, Y. Zeng, Z. Xu, Z. Yang, Three-layer model for vertical velocity distribution in open channel flow with submerged rigid vegetation, Advances in Water Resources 32 (4) (2009) 487-492. http://dx.doi.org/10.1016/j.advwatres.2008.11.014

[54] D. Liu, P. Diplas, J. D. Fairbanks, C. C. Hodges, An experimental study of flow through rigid vegetation, Journal of Geophysical Research: Earth Surface 113 (F4) (2008) F04015, http://dx.doi.org/10.1029/2008JF001042

[55] M. Ghisalberti, H. Nepf, The structure of the shear layer in flows over rigid and flexible canopies, Environmental Fluid Mechanics 6 (3) (2006) 277-301, http://dx.doi.org/10.1007/s10652-006-0002-4

[56] T. Stoesser, G. Salvador, W. Rodi, P. Diplas, Large eddy simulation of turbulent flow through submerged vegetation, Transport in Porous Media 78 (3) (2009) 347-365. http://dx.doi.org/10.1007/s11242-009-9371-8

[57] A. A. Jordanova, C. S. James, Experimental study of bed load transport through emergent vegetation, Journal of Hydraulic Engineering 129 (6) (2003) 474-478. http://dx.doi.org/10.1061/(ASCE)0733-9429(2003)129:6(474)

[58] U. C. Kothyari, H. Hashimoto, K. Hayashi, Effect of tall vegetation on sediment transport by channel flows, Journal of Hydraulic Research 47 (6) (2009) 700-710. http://dx.doi.org/10.3826/jhr.2009.3317

[59] F. López, M. García, Open-channel flow through simulated vegetation: Suspended sediment transport modeling, Water Resources Research 34 (9) (1998) 2341-2352, http://dx.doi.org/10.1029/98WR01922

[60] R. G. Sharpe, C. S. James, Deposition of sediment from suspension in emergent vegetation, Water SA 32 (2) (2007) 211-218. http://dx.doi.org/10.4314/wsa.v32i2.5244

[61] E. M. Yager, M. W. Schmeeckle, The influence of vegetation on turbulence and bed load transport, Journal of Geophysical Research: Earth Surface 118 (3) (2013) 1585-1601. http://dx.doi.org/10.1002/jgrf.20085

[62] E. Pasche, G. Rouvé, Overbank flow with vegetatively roughened flood plains, Journal of Hydraulic Engineering 111 (9) (1985) 1262-1278. http://dx.doi.org/10.1061/(ASCE)0733-9429(1985)111:9(1262)

[63] C. Thornton, S. Abt, C. Morris, J. Fischenich, Calculating shear stress at channel-overbank interfaces in straight channels with vegetated floodplains, Journal of Hydraulic Engineering 126 (12) (2000) 929-936. http://dx.doi.org/10.1061/(ASCE)0733-9429(2000)126:12(929)

[64] C. E. Oldham, J. J. Sturman, The effect of emergent vegetation on convective flushing in shallow wetlands: Scaling and experiments, Limnology and Oceanography 46 (6) (2001) 1486-1493. http://dx.doi.org/10.4319/lo.2001.46.6.1486

[65] T. Wynn, S. Mostaghimi, The effects of vegetation and soil type on stream bank erosion, Southwestern Virginia, USA, JAWRA Journal of the American Water Resources Association 42 (1) (2006) 69-82. http://dx.doi.org/10.1111/j.1752-1688.2006.tb03824.x

[66] M. McBride, W. C. Hession, D. M. Rizzo, D. M. Thompson, The influence of riparian vegetation on near-bank turbulence: a flume experiment, Earth Surface Processes and Landforms 32 (13) (2007) 2019-2037. http://dx.doi.org/10.1002/esp.1513

[67] B. L. White, H. M. Nepf, A vortex-based model of velocity and shear stress in a partially vegetated shallow channel, Water Resources Research 44 (1) (2008) W01412, doi:10.1029/2006WR005651. http://dx.doi.org/10.1029/2006WR005651

[68] M. Sanjou, I. Nezu, S. Suzuki, K. Itai, Turbulence structure of compound open-channel flows with one-line emergent vegetation, Journal of Hydrodynamics, Ser. B 22 (5, Supplement 1) (2010) 577-581. http://dx.doi.org/10.1016/S1001-6058(09)60255-9

[69] F. Jahra, Y. Kawahara, F. Hasegawa, H. Yamamoto, Flow-vegetation interaction in a compound open channel with emergent vegetation, International Journal of River Basin Management 9 (3-4) (2011) 247-256. http://dx.doi.org/10.1080/15715124.2011.642379

[70] T. Takemura, N. Tanaka, Flow structures and drag characteristics of a colony-type emergent roughness model mounted on a at plate in uniform flow, Fluid Dynamics Research 39 (9-10) (2007) 694-710. http://dx.doi.org/10.1016/j.fluiddyn.2007.06.001

[71] A. Nicolle, I. Eames, Numerical study of flow through and around a circular array of cylinders, Journal of Fluid Mechanics 679 (2011) 1-31. http://dx.doi.org/10.1017/jfm.2011.77

[72] L. Zong, H. Nepf, Vortex development behind a finite porous obstruction in a channel, Journal of Fluid Mechanics 691 (2012) 368-391. http://dx.doi.org/10.1017/jfm.2011.479

[73] H. S. Kim, I. Kimura, Y. Shimizu, Bed morphological changes around a finite patch of vegetation, Earth Surface Processes and Landforms 40 (3) (2015) 375-388. http://dx.doi.org/10.1002/esp.3639

[74] A. Vargas-Luna, A. Crosato, W. Uijttewaal, Effects of vegetation on flow and sediment transport: comparative analyses and validation of predicting models, Earth Surface Processes and Landforms 40 (2) (2015) 157-176. http://dx.doi.org/10.1002/esp.3633

[75] J. T. Dijkstra, R. E. Uittenbogaard, Modeling the interaction between flow and highly flexible aquatic vegetation, Water Resources Research 46 (2010) W12547, http://dx.doi.org/10.1029/2010WR009246

[76] W. Wu, F. D. Shields Jr, S. J. Bennett, S. S. Y. Wang, A depth-averaged two-dimensional model for flow, sediment transport, and bed topography in curved channels with riparian vegetation, Water Resources Research 41 (3) (2005) W03015, http://dx.doi.org/10.1029/2004WR003730

[77] N. Cheng, Calculation of drag coefficient for arrays of emergent circular cylinders with pseudo-fluid model, Journal of Hydraulic Engineering 139 (6) (2013) 602-611. http://dx.doi.org/10.1061/(ASCE)HY.1943-7900.0000722

[78] M. J. Baptist, L. V. van den Bosch, J. T. Dijkstra, S. Kapinga, Modelling the effects of vegetation on flow and morphology in rivers, Archiv für Hydrobiologie Supplement 155/14, Large Rivers 15 (1-4) (2003) 339-357. http://dx.doi.org/10.1127/lr/15/2003/339.

[79] H. M. Nepf, E. R. Vivoni, Flow structure in depth-limited, vegetated flow, Journal of Geophysical Research 105 (C12) (2000) 28.547-28.557. http://dx.doi.org/10.1029/2000JC900145.

[80] V. Neary, S. Constantinescu, S. Bennett, P. Diplas, Effects of vegetation on turbulence, sediment transport, and stream morphology, Journal of Hydraulic Engineering 138 (9) (2012) 765-776. http://dx.doi.org/10.1061/(ASCE)HY.1943-7900.0000168.

[81] M. Luhar, H. M. Nepf, From the blade scale to the reach scale: A characterization of aquatic vegetative drag, Advances in Water Resources 51 (2013) 305-316. http://dx.doi.org/10.1016/j.advwatres.2012.02.002.

[82] E. Murphy, M. Ghisalberti, H. Nepf, Model and laboratory study of dispersion in flows with submerged vegetation, Water Resources Research 43 (5) (2007) W05438, http://dx.doi.org/10.1029/2006WR005229

[83] J. D. Shucksmith, J. B. Boxall, I. Guymer, Determining longitudinal dispersion coefficients for submerged vegetated flow, Water Resources Research 47 (10) (2011) W10516, http://dx.doi.org/10.1029/2011WR010547.

[84] V. A. Vanoni, N. H. Brooks, Laboratory studies of the roughness and suspended load of alluvial streams (1957).

[85] P. Byishimo, Effects of variable discharge on width formation and cross-sectional shape of sinuous rivers, Master's thesis, UNESCO-IHE, Institute for Water Education, Delft, The Netherlands (2014).

[86] K. P. Dulal, K. Kobayashi, Y. Shimizu, G. Parker, Numerical computation of free meandering channels with the application of slump blocks on the outer bends, Journal of Hydro-environment Research 3 (4) (2010) 239-246. http://dx.doi.org/10.1016/j.jher.2009.10.012

[87] \T. B. Abbe, D. R. Montgomery, Patterns and processes of wood debris accumulation in the Queets river basin, Washington, Geomorphology 51 (1-3) (2003) 81-107. http://dx.doi.org/10.1016/S0169-555X(02)00326-4

[88] C. J. Brummer, T. B. Abbe, J. R. Sampson, D. R. Montgomery, Influence of vertical channel change associated with wood accumulations on delineating channel migration zones, Washington, USA, Geomorphology 80 (3-4) (2006) 295-309. http://dx.doi.org/10.1016/j.geomorph.2006.03.002

[89] B. D. Collins, D. R. Montgomery, K. L. Fetherston, T. B. Abbe, The floodplain large-wood cycle hypothesis: A mechanism for the physical and biotic structuring of temperate forested alluvial valleys in the north pacific coastal ecoregion, Geomorphology 139-140 (0) (2012) 460-470. http://dx.doi.org/10.1016/j.geomorph.2011.11.011

[90] A. M. Gurnell, G. E. Petts, D. M. Hannah, B. P. G. Smith, P. J. Edwards, J. Kollmann, J. V. Ward, K. Tockner, Riparian vegetation and island formation along the gravel-bed fiume Tagliamento, Italy, Earth Surface Processes and Landforms 26 (1) (2001) 31-62. http://dx.doi.org/10.1002/1096-9837(200101)26:1<31::AID-ESP155>3.0.CO;2-Y

[91] J. E. O'Connor, M. A. Jones, T. L. Haluska, Flood plain and channel dynamics of the Quinault and Queets rivers, Washington, USA, Geomorphology 51 (1-3) (2003) 31-59, interactions between Wood and Channel Forms and Processes. http://dx.doi.org/10.1016/S0169-555X(02)00324-0

[92] A. M. Gurnell, G. E. Petts, Trees as riparian engineers: the Tagliamento river, Italy, Earth Surface Processes and Landforms 31 (12) (2006) 1558-1574. http://dx.doi.org/10.1002/esp.1342

[93] D. Corenblit, J. Steiger, E. Tabacchi, Biogeomorphologic succession dynamics in a mediterranean river system, Ecography 33 (6) (2010) 1136-1148. http://dx.doi.org/10.1111/j.1600-0587.2010.05894.x.

[94] G. C. Nanson, Point bar and floodplain formation of the meandering Beatton river, Northeastern British Columbia, Canada, Sedimentology 27 (1) (1980) 3-29. http://dx.doi.org/10.1111/j.1365-3091.1980.tb01155.x

[95] N. Struiksma, K. W. Olesen, C. Flokstra, H. J. De Vriend, Bed deformation in curved alluvial channels, Journal of Hydraulic Research 23 (1) (1985) 57-79. http://dx.doi.org/10.1080/00221688509499377

[96] R. Bagnold, An approach to the sediment transport problem from general physics, US Geological Survey Professional Paper 422-I, 37 pages (1966).

[97] S. Ikeda, Lateral bed slope transport on side slopes, Journal of the Hydraulics Division ASCE 108 (11) (1982) 1369-1373.

[98] E. Meyer-Peter, R. Müller, Formulas for bed load transport, in: Proceedings of the 2nd IAHR Congress, Stockholm, Sweden, 2: 39-64, (1948).

[99] G. Galappatti, C. B. Vreugdenhil, A depth-integrated model for suspended sediment transport, Journal of Hydraulic Research 23 (4) (1985) 359-377. http://dx.doi.org/10.1080/00221688509499345

[100] M. van der Wegen, J. A. Roelvink, Long-term morphodynamic evolution of a tidal embayment using a two-dimensional, process-based model, Journal of Geophysical Research: Oceans 113 (C03016) (2008). http://dx.doi.org/10.1029/2006JC003983

[101] M. J. Baptist, J. F. de Jong, Modelling the influence of vegetation on the morphology of the Allier, France, in: H. A. et al. (Ed.), Final COST 626 Meeting, Silkeborg, Denmark, 19-20 May 2005, 2005, pp. 15-22.

[102] A. Crosato, E. Mosselman, Simple physics-based predictor for the number of river bars and the transition between meandering and braiding, Water Resources Research 45 (2009), W03424. http://dx.doi.org/10.1029/2008WR007242

[103] M. R. Gibling, N. S. Davies, Palaeozoic landscapes shaped by plant evolution, Nature Geoscience 5 (2) (2012) 99-105. http://dx.doi.org/10.1038/ngeo1376

[104] E. Facchini, Morphological aspects of cyclic rejuvenation of the Ewijkse plaat, the Netherlands, Master's thesis, University of Florence, Faculty of Engineering, Florence, Ityaly, and UNESCO-IHE, Delft, the Netherlands (March 2009).

[105] E. Facchini, A. Crosato, E. Kater, La modellazione numerica nei progetti di riqualificazione fluviale: il caso Ewijkse plaat, paesi bassi, in: Riqualificazione Fluviale, ECRR-CIRF, No. 2/2009: p. 6773 (in Italian), (2009).

[106] A. Montes Arboleda, A. Crosato, H. Middelkoop, Reconstructing the early 19th-century Waal river by means of a 2d physics-based numerical model, Hydrological Processes 24 (25) (2010) 3661-3675. http://dx.doi.org/10.1002/hyp.7804

[107] A. Bouwman, De netto sedimentatie op de ewijkse plaat berekend met de krigingmethode, Technical report 99.118X, Rijksinstituut voor Integral Zoetwaterbeheer en Afvalwaterbehandeling (RIZA) (in Dutch) (1999).

[108] G. Geerling, E. Kater, C. van den Brink, M. Baptist, A. Ragas, A. Smits, Nature rehabilitation by floodplain excavation: The hydraulic effect of 16 years of sedimentation and vegetation succession along the Waal river, (NL), Geomorphology 99 (14) (2008) 317-328. http://dx.doi.org/10.1016/j.geomorph.2007.11.011

[109] N. E. M. Asselman, Suspended sediments in the river rhine, Ph.D. thesis, University of Utrecht, The Netherlands (1997).

[110] H. Middelkoop, Reconstructing floodplain sedimentation rates from heavy metal profiles by inverse modelling, Hydrological Processes 16 (1) (2002) 47-64. http://dx.doi.org/10.1002/hyp.283

[111] W. van Vuuren, Verdeling zomer- en winterhoogwaters voor de rijntakken in de periode 1770-2004, In: Memo WRR 2005-012, to: E. Van Velzen (in Dutch) (2005).

[112] G. Maas, H. Wolfert, M. Schoor, H. Middelkoop, Classificatie van rivier trajecten en kansrijkdom voor ecotopen, Report 552, DLO-490 Staring Centrum, Wageningen, the Netherlands (in Dutch) (1997).

[113] J. Pizzuto, Sediment diffusion during overbank flows, Sedimentology 34 (2) (1987) 301-317. http://dx.doi.org/10.1111/j.1365-3091.1987.tb00779.x

[114] T. J. Coulthard, Effects of vegetation on braided stream pattern and dynamics, Water Resources Research 41 (2005) W04003, http://dx.doi.org/10.1029/2004WR003201

[115] S. Temmerman, T. Bouma, J. Van de Koppel, D. Van der Wal, M. De Vries, P. Herman, Vegetation causes channel erosion in a tidal landscape, Geology 35 (7) (2007) 631-634. http://dx.doi.org/10.1130/G23502A.1

[116] T. Fischer-Antze, T. Stoesser, P. Bates, N. Olsen, 3D numerical modelling of open-channel flow with submerged vegetation, Journal of Hydraulic Research 39 (3) (2001) 303-310. http://dx.doi.org/10.1080/00221680109499833

[117] T. Helmiö, Unsteady 1D flow model of compound channel with vegetated floodplains, Journal of Hydrology 269 (1-2) (2002) 89-99. http://dx.doi.org/10.1016/S0022-1694(02)00197-X

[118] T. Stoesser, C.A.M.E Wilson, P.D. Bates, A. Dittrich, Application of a 3D numerical model to a river with vegetated floodplains, Journal of Hydroinformatics 5 (2003) 99-112.

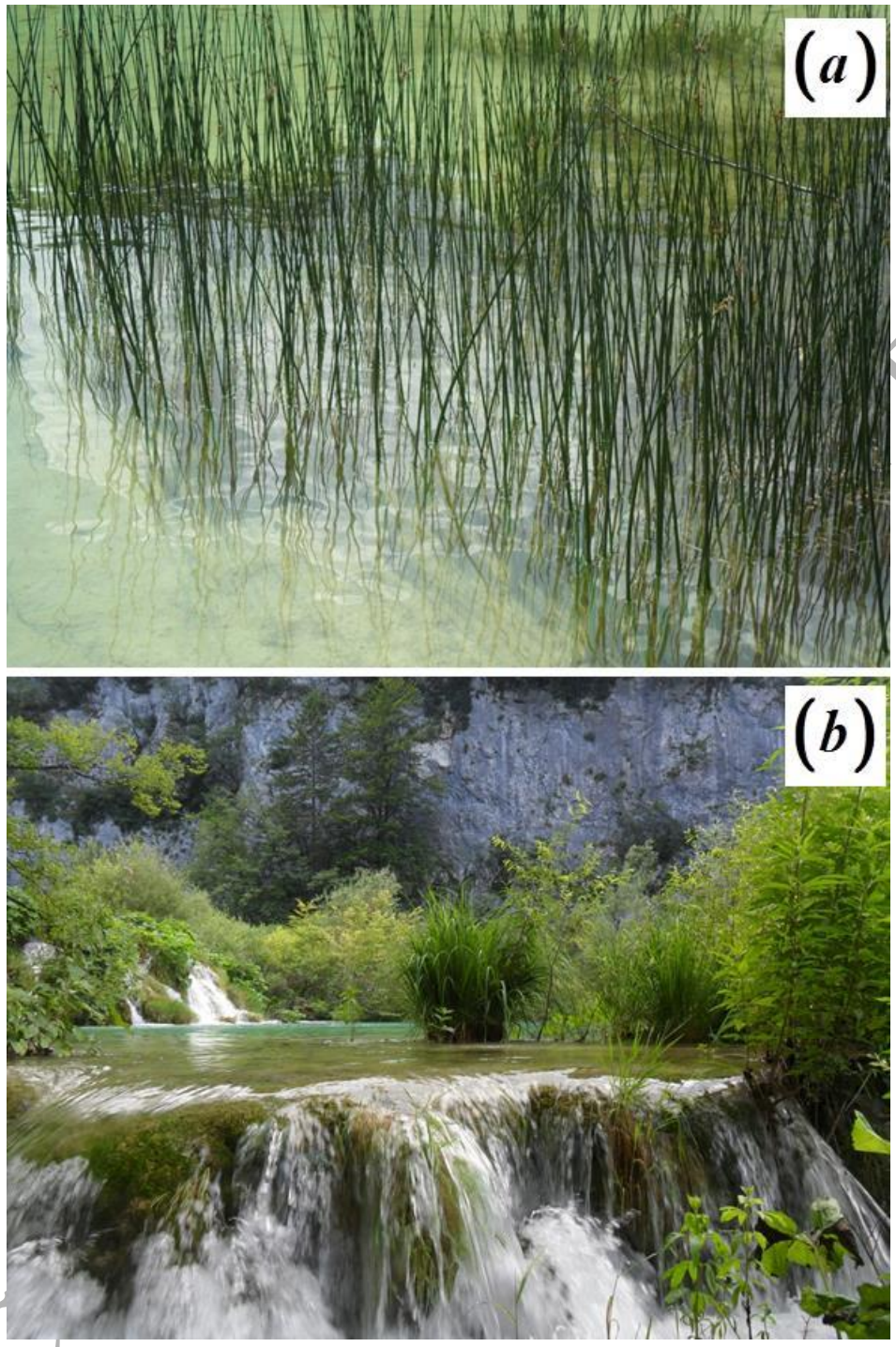

Figure 1. Comparison of geometric characteristics of plants: (a) Uniform, cylindrical and leafless; and (b) Irregular, with high variability in density and foliage. Photo taken at Plitvice, Croatia.

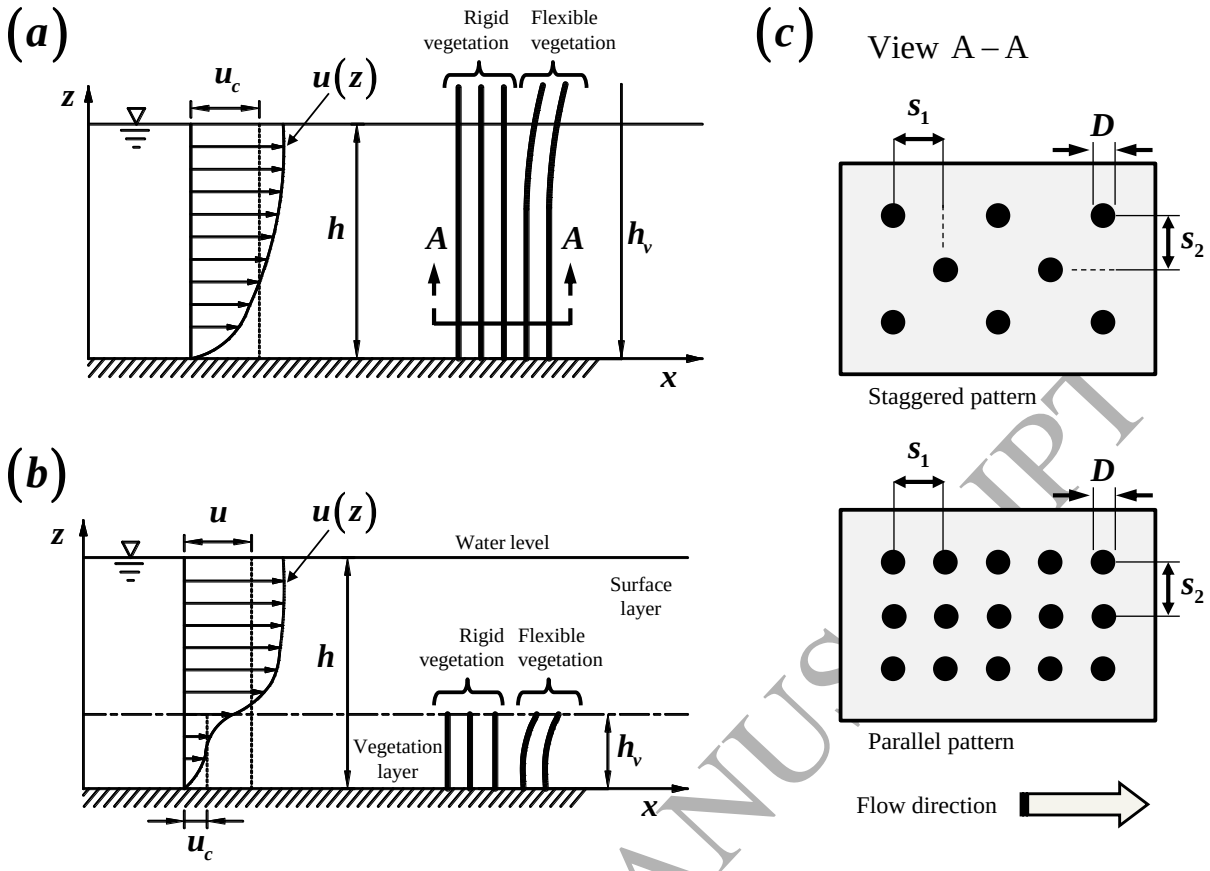

Figure 2. Main characteristics of rigid and flexible vegetation in open channels. Left: side view of emergent vegetation (above) and submerged vegetation (below), Adapted from: Wu and He [10]. Right: plan view of staggered and parallel patterns. Variables and units shown in the notation section.

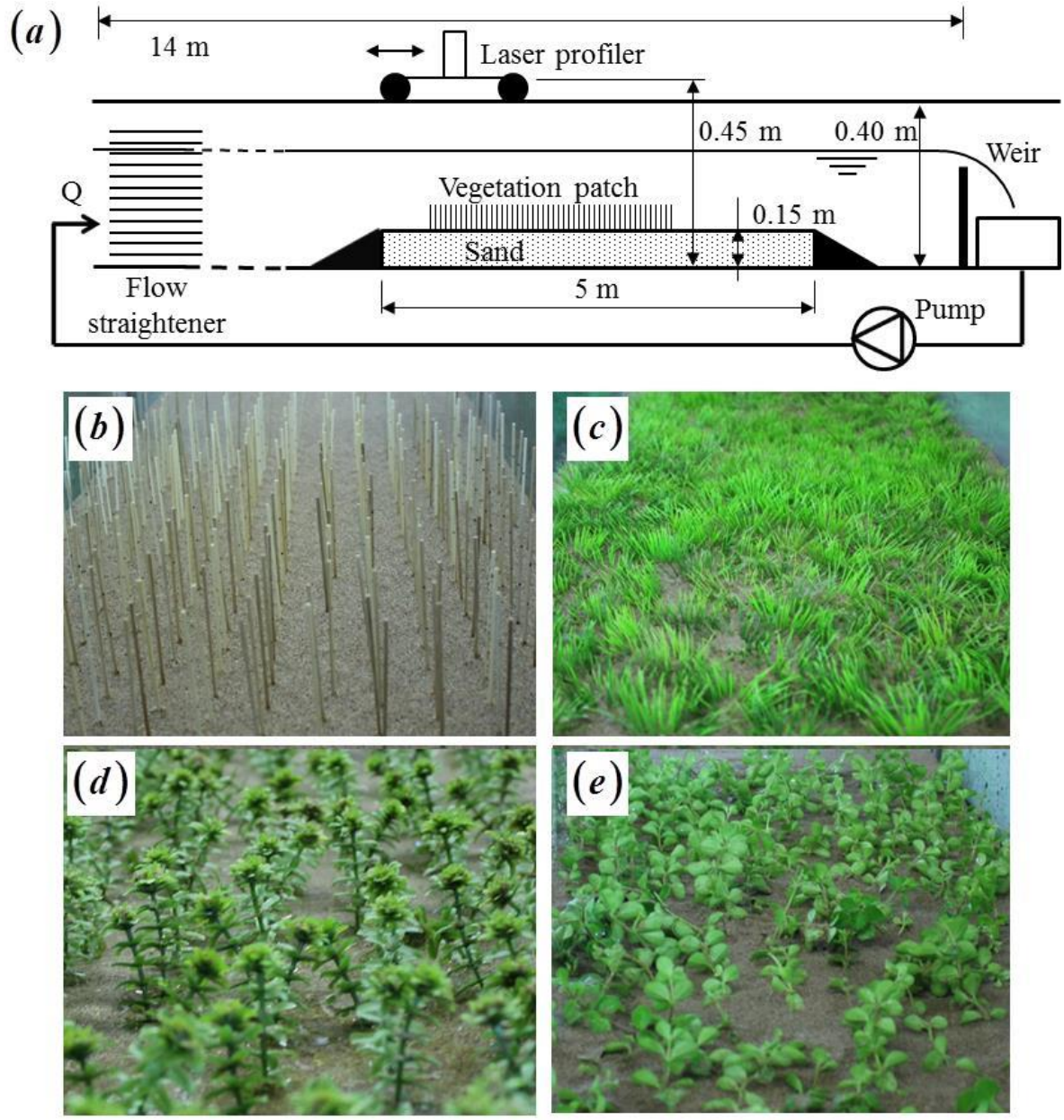

Figure 3. Experimental setup for Flume No. 1. (a) and vegetation arrays used: (b) Rigid (Wooden) sticks [Test W11], (c) Artificial Grass [Test G2], (d) Artificial with Leaves (*Egeria densa*) [Test ED3], (e) Real (*Peperomia rotundifolia*) [Test R2]. Vegetation properties are presented in Table 1.

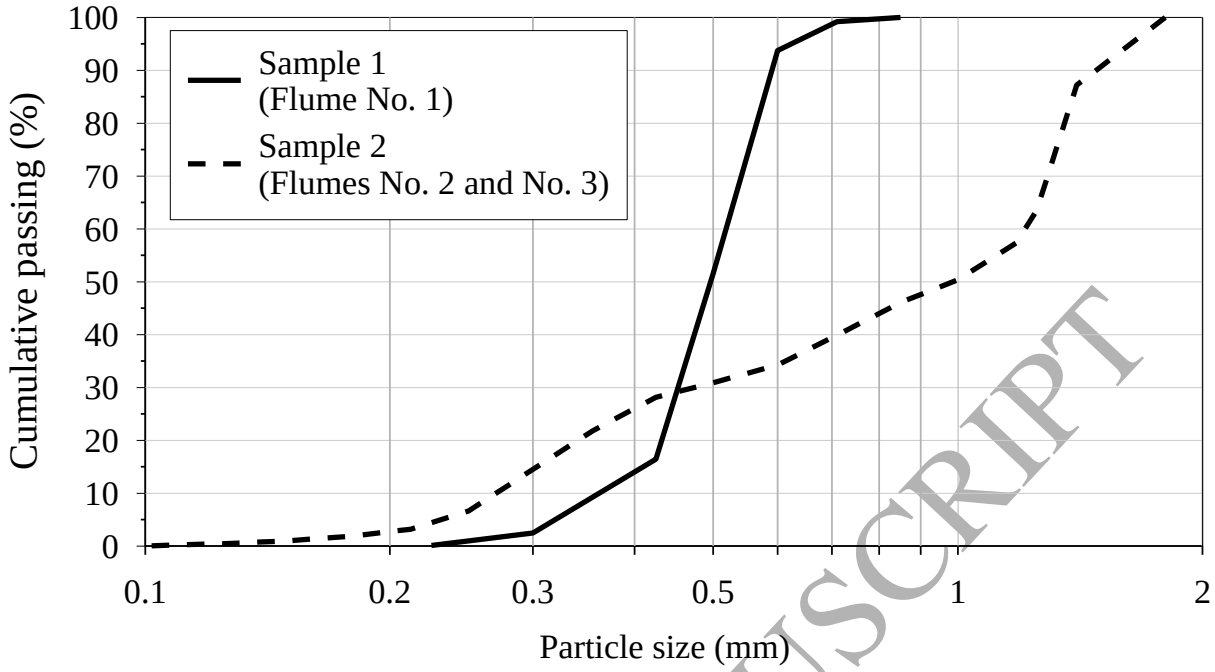

Figure 4. Sediments used in the laboratory experiments.

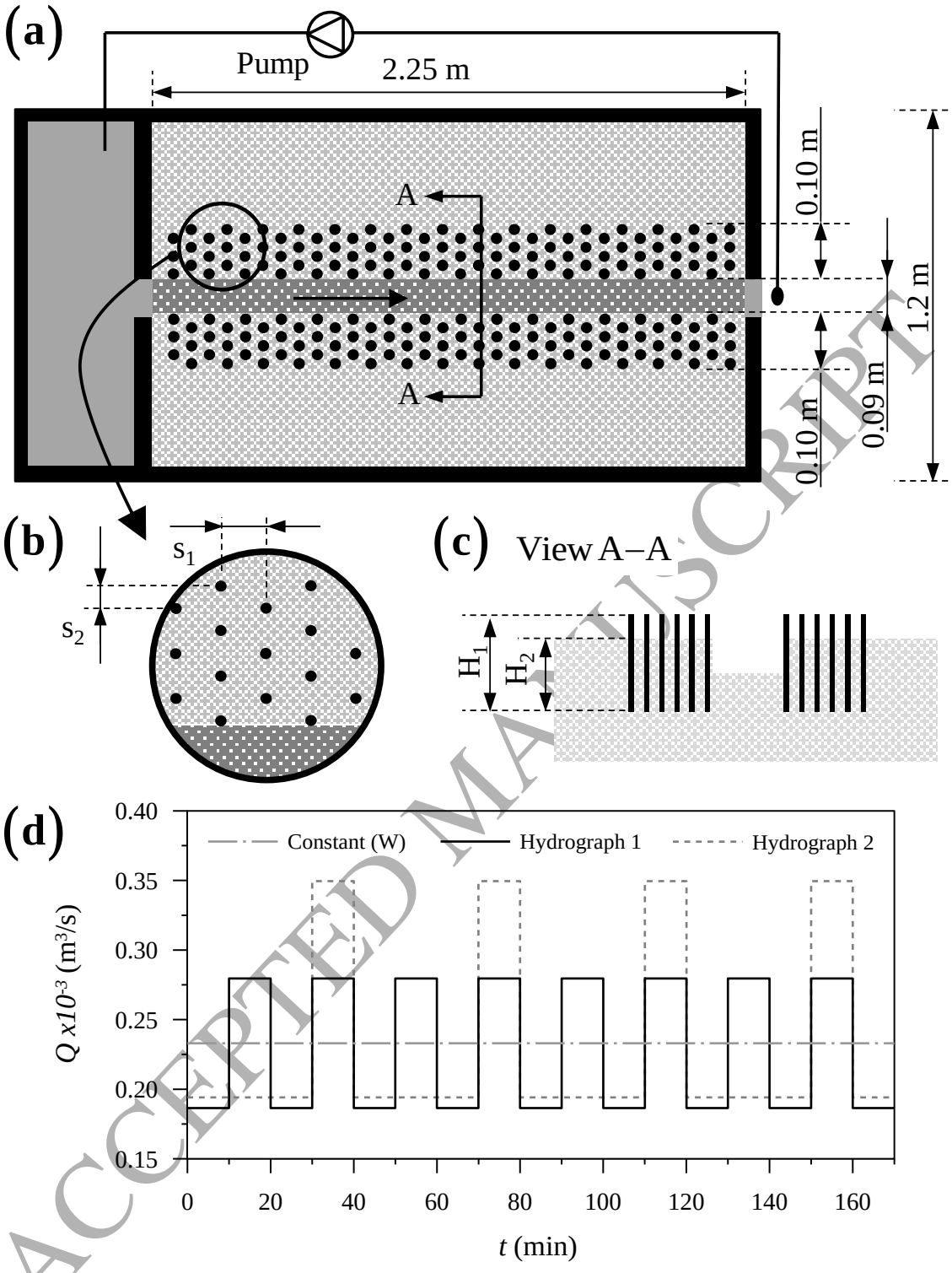

Figure 5. Experimental setup for Flume No. 2. (a) Plan view, (b) Vegetation distribution on the floodplains, (c) Typical cross-section, and (d) Hydrographs used in the experiments. Initial bed slope = 0.01 m/m.

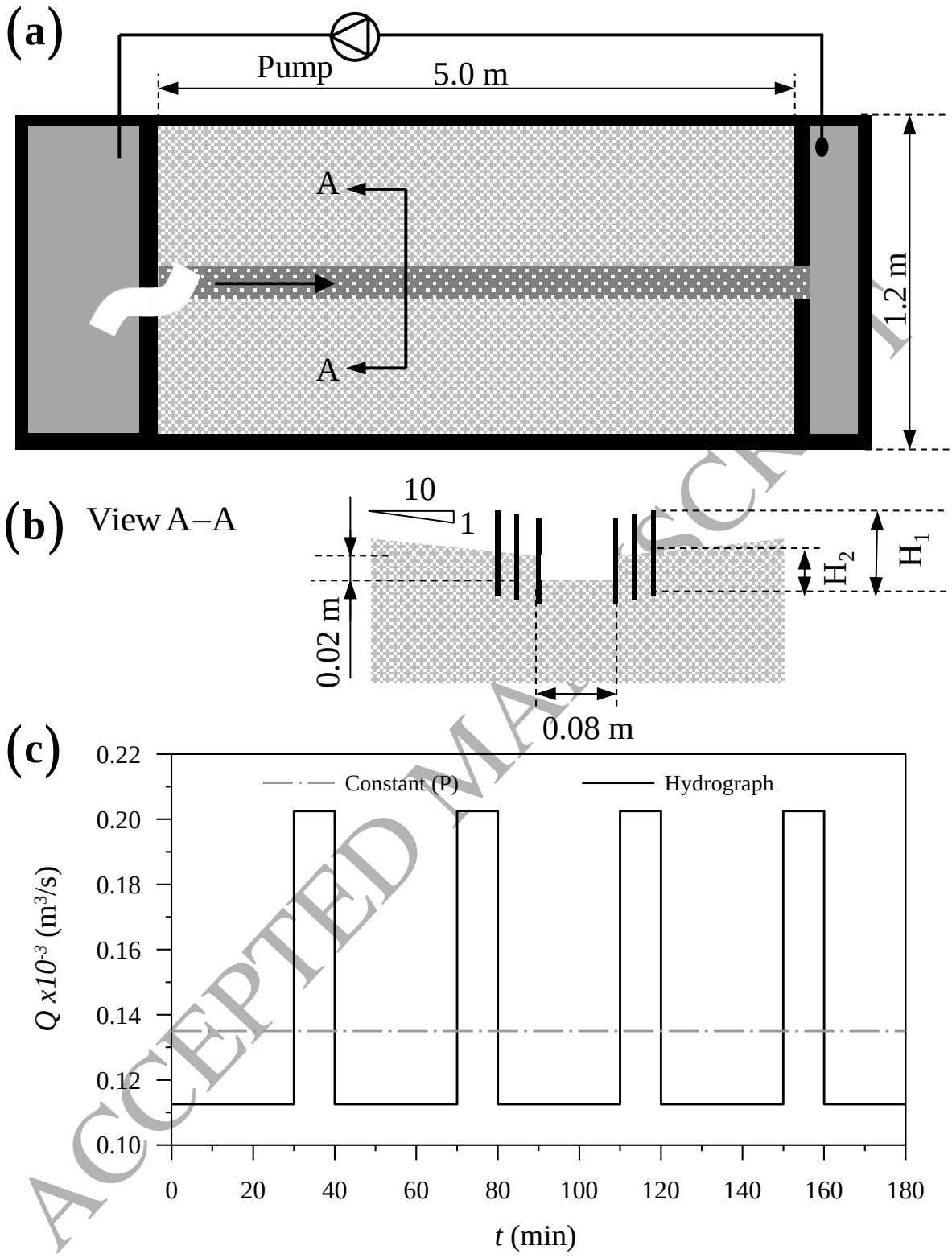

Figure 6. Experimental setup for Flume No. 3. (a) Plan view, (b) Typical cross-section, and (c) Hydrographs used in the experiments. Initial bed slope = 0.01 m/m.

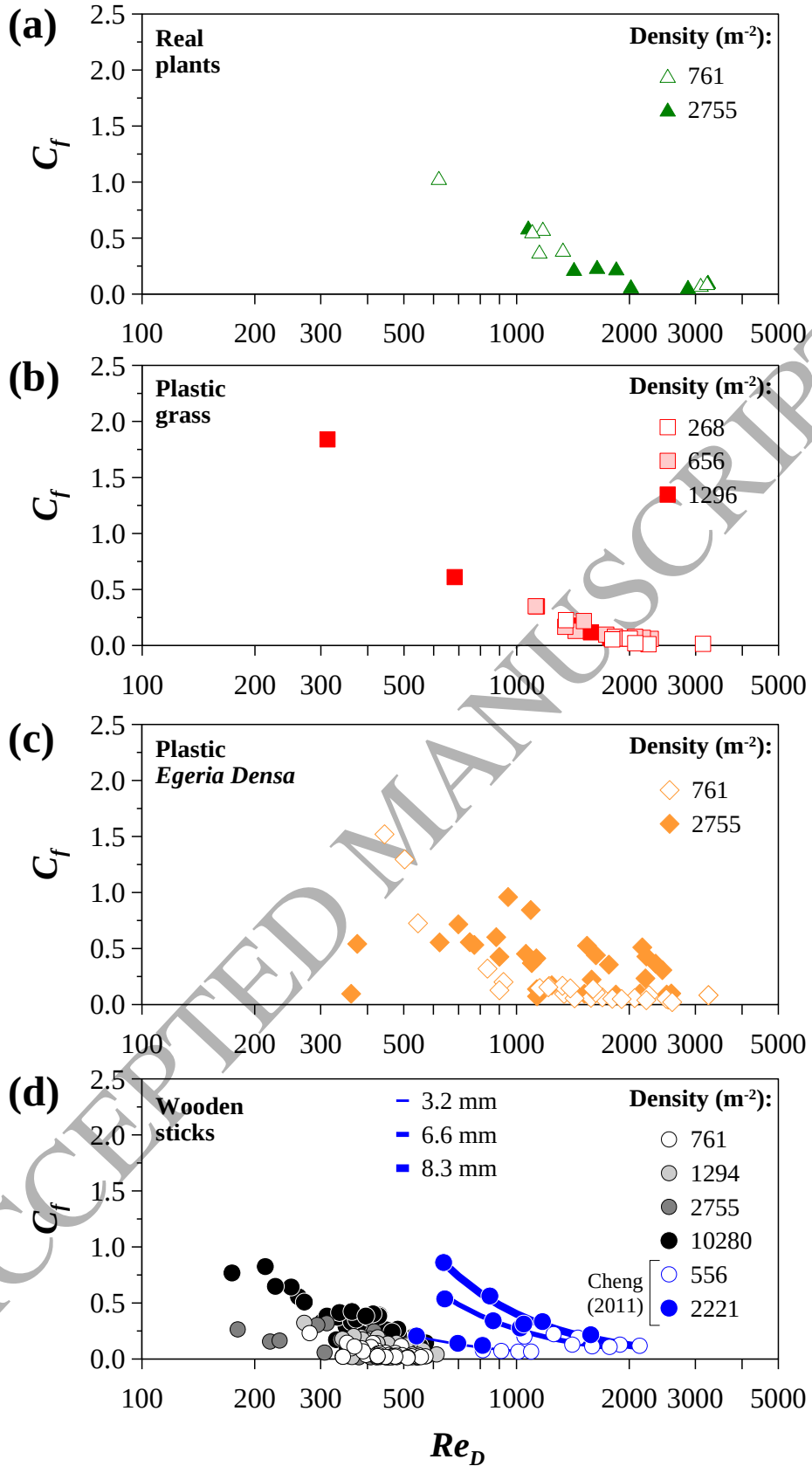

Figure 7. Friction coefficient (C_f) as a function of the element Reynolds number (Re_D) for: (a) Real plants [h/h_v: 2.0 - 3.6], (b) Plastic grass [h/h_v: 4.7 - 8.7], (c) Plastic *Egeria Densa* [h/h_v: 1.8 - 8.8], and (d) Wooden sticks [h/h_v: 1.5 - 7.8] and cylindrical rods by Cheng [31] [h/h_v: 1.3 - 2.0]. Vegetation properties are listed in Table 1.

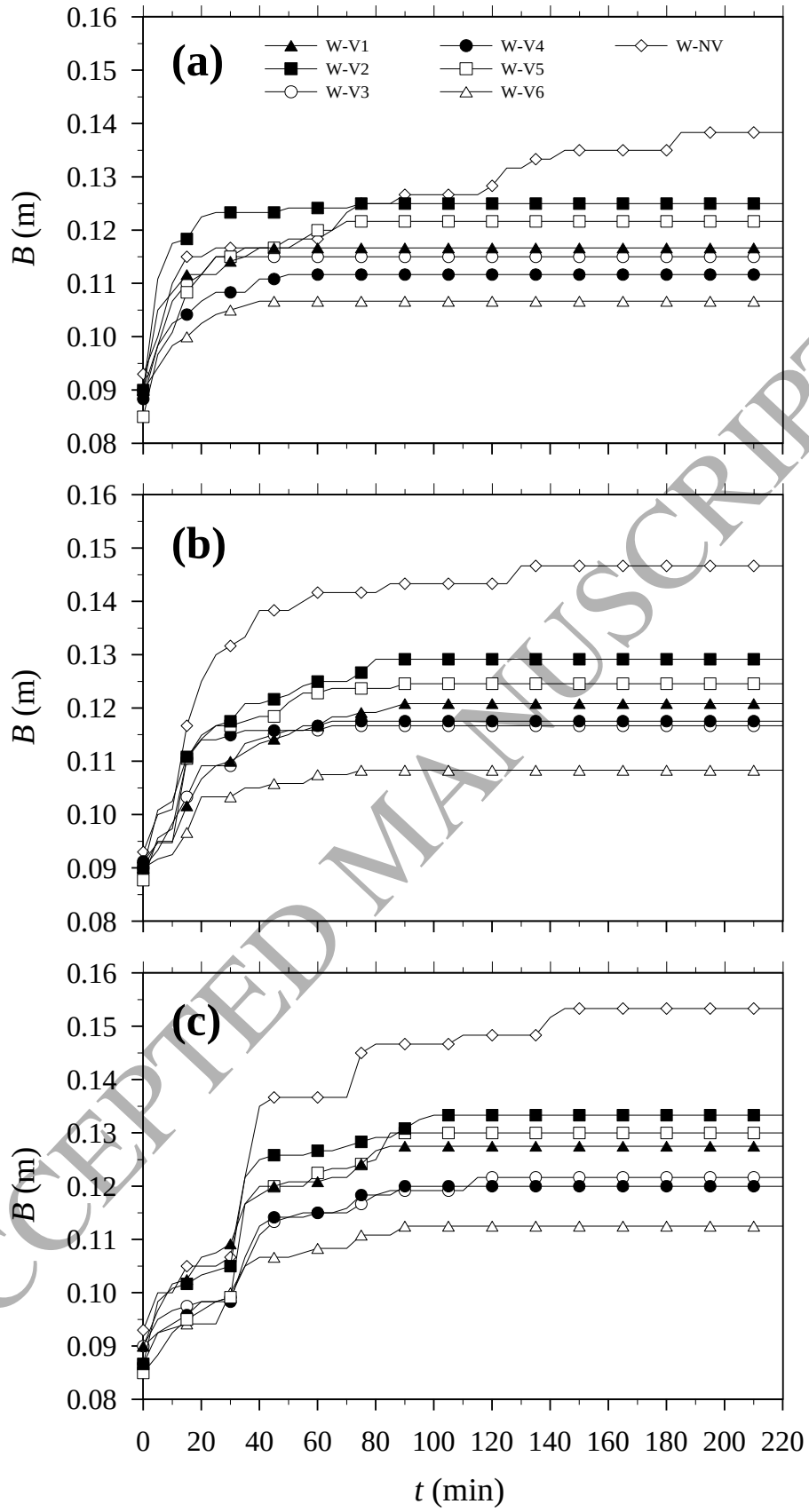

Figure 8. Channel-width (*B*) variation with time in the experiments carried out in Flume No. 2 for: (a) Constant discharge, (b) Hydrograph 1, and (c) Hydrograph 2. The vegetation properties are summarized in Table 2 and the hydrographs are shown in Fig. 5d.

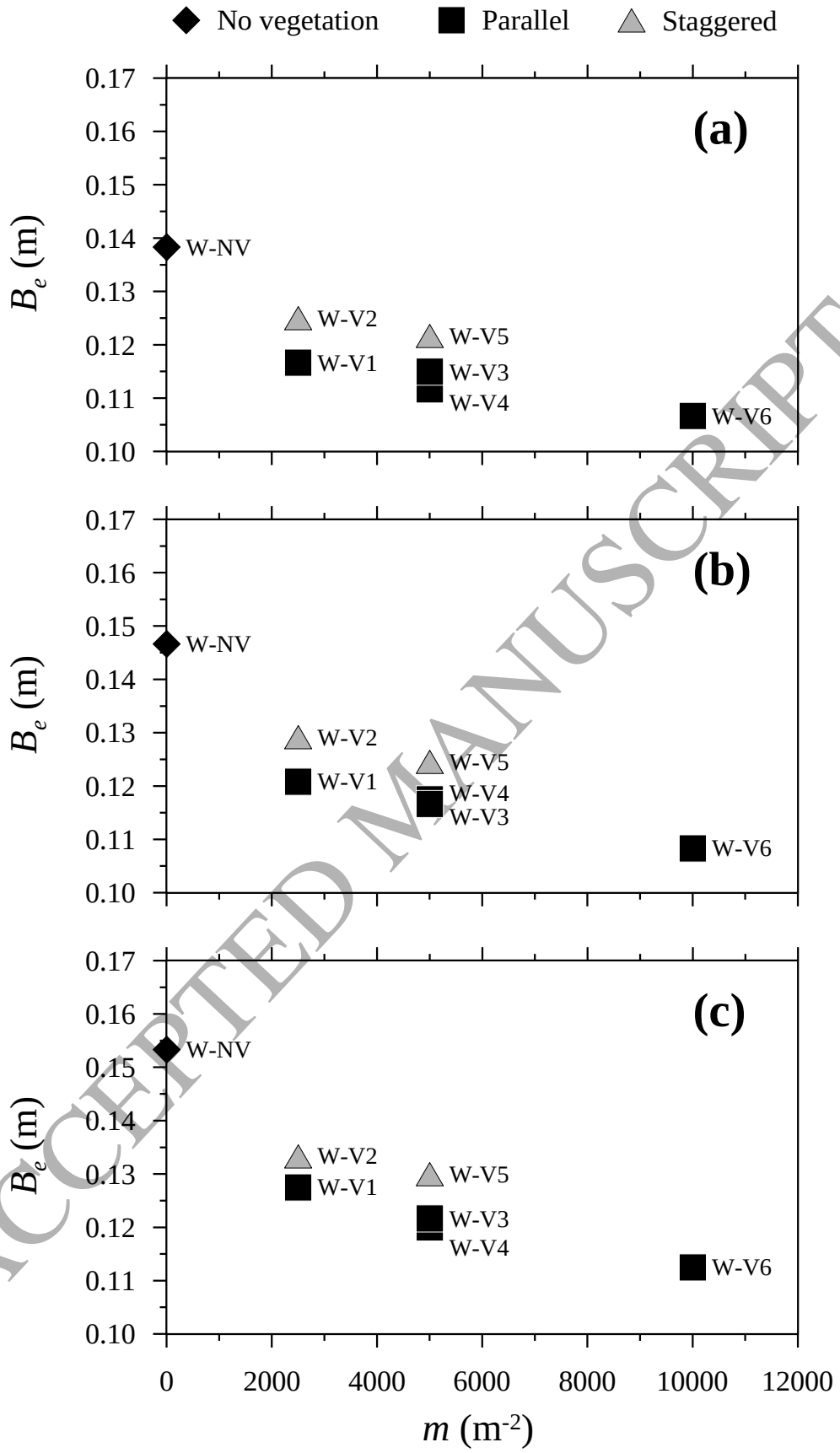

Figure 9. Equilibrium channel width (B_e) for the experiments carried out in Flume No. 2 for: (a) Constant discharge, (b) Hydrograph 1, and (c) Hydrograph 2. The vegetation properties used are summarized in Table 2 and the hydrographs are shown in Fig. 5d.

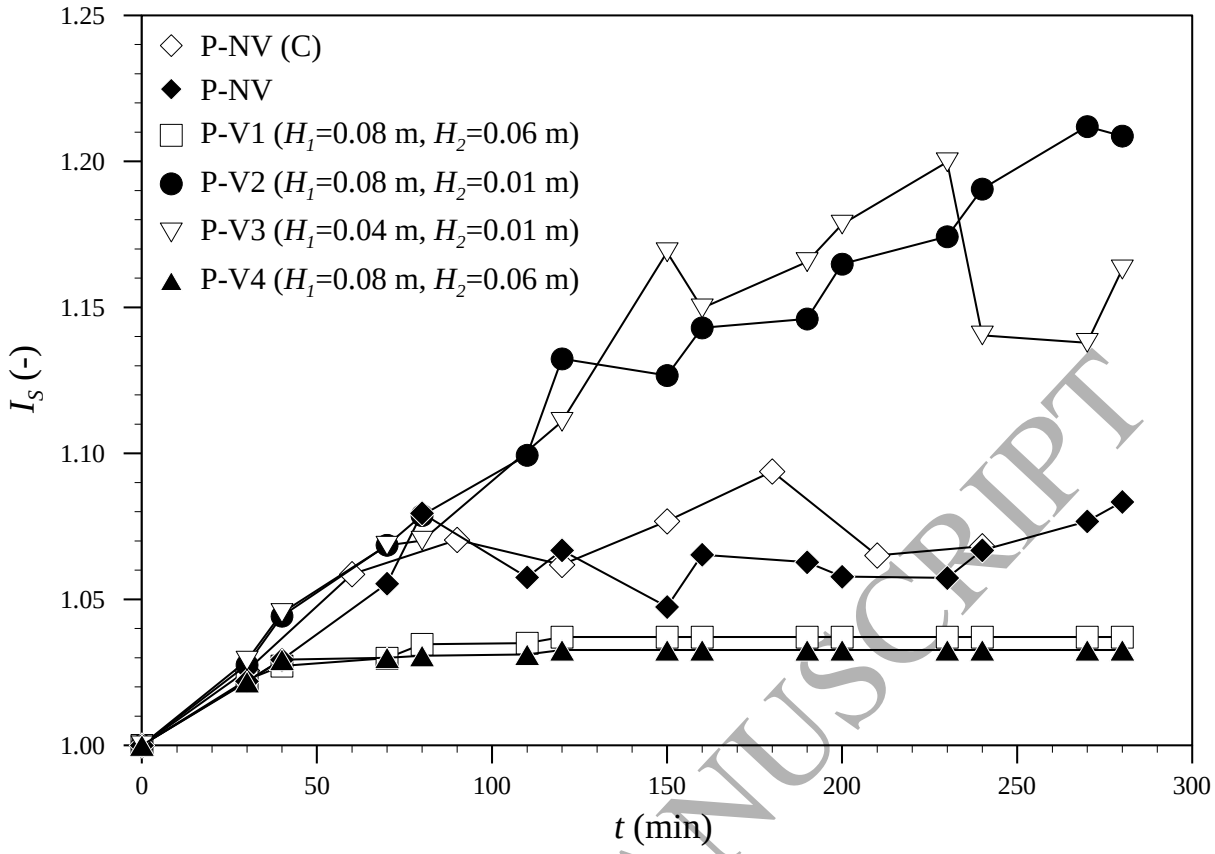

Figure 10. Channel sinuosity (I_S) variation with time for the experiments carried out in Flume No. 3. The letter C indicates the experiment that was performed with constant discharge. The vegetation properties used are summarized in Table 3 and the hydrographs are shown in Fig. 6c.

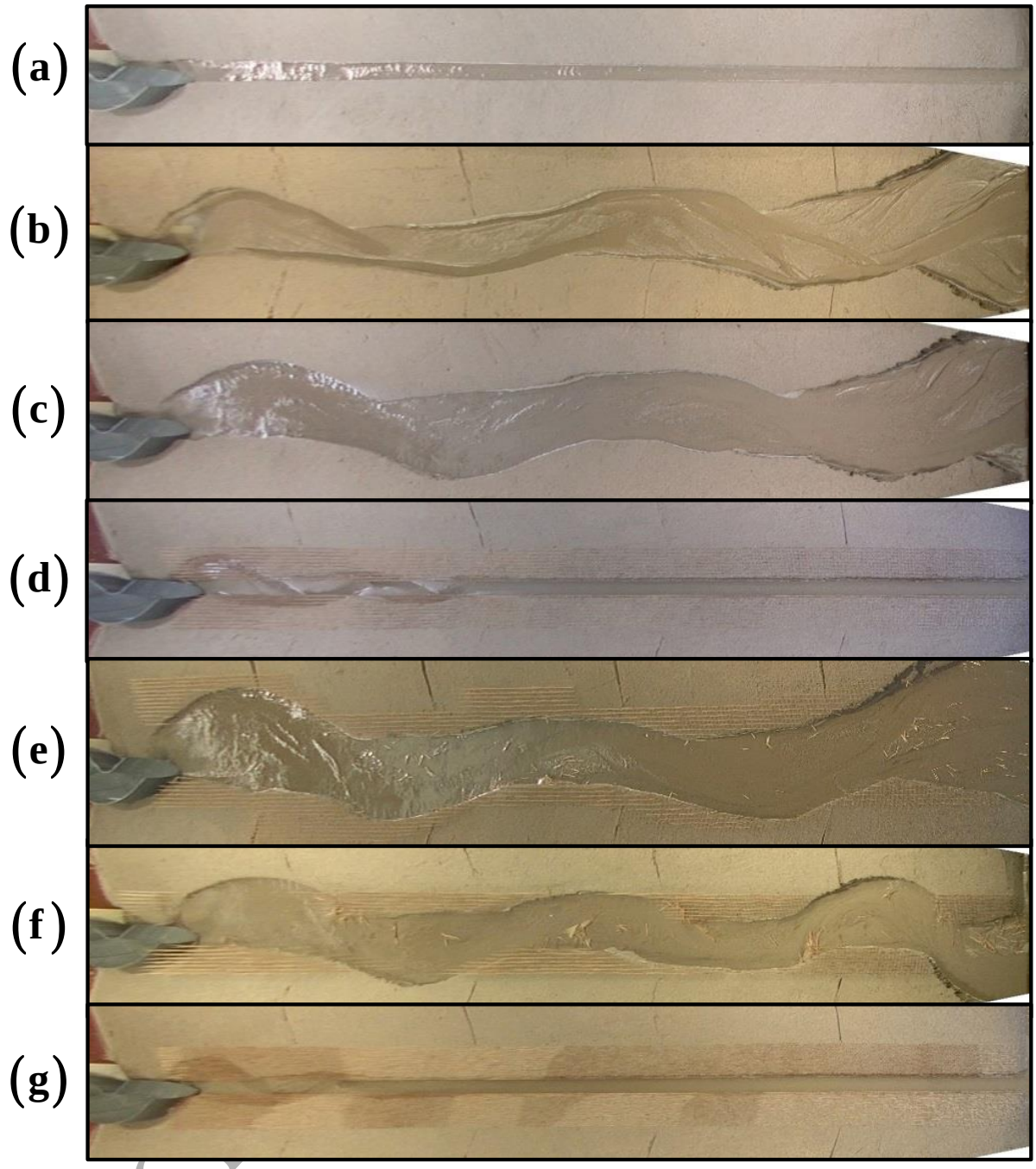

Figure 11. Common initial configuration (a) and channel planform after 240 minutes for the experiments in Flume No. 3: (b) Test P-NV (constant discharge); (c) Test P-NV (variable discharge); (d) Test P-V1; (e) Test P-V2; (f) Test P-V3; (g) Test P-V4. Vegetation properties are listed in Table 3.

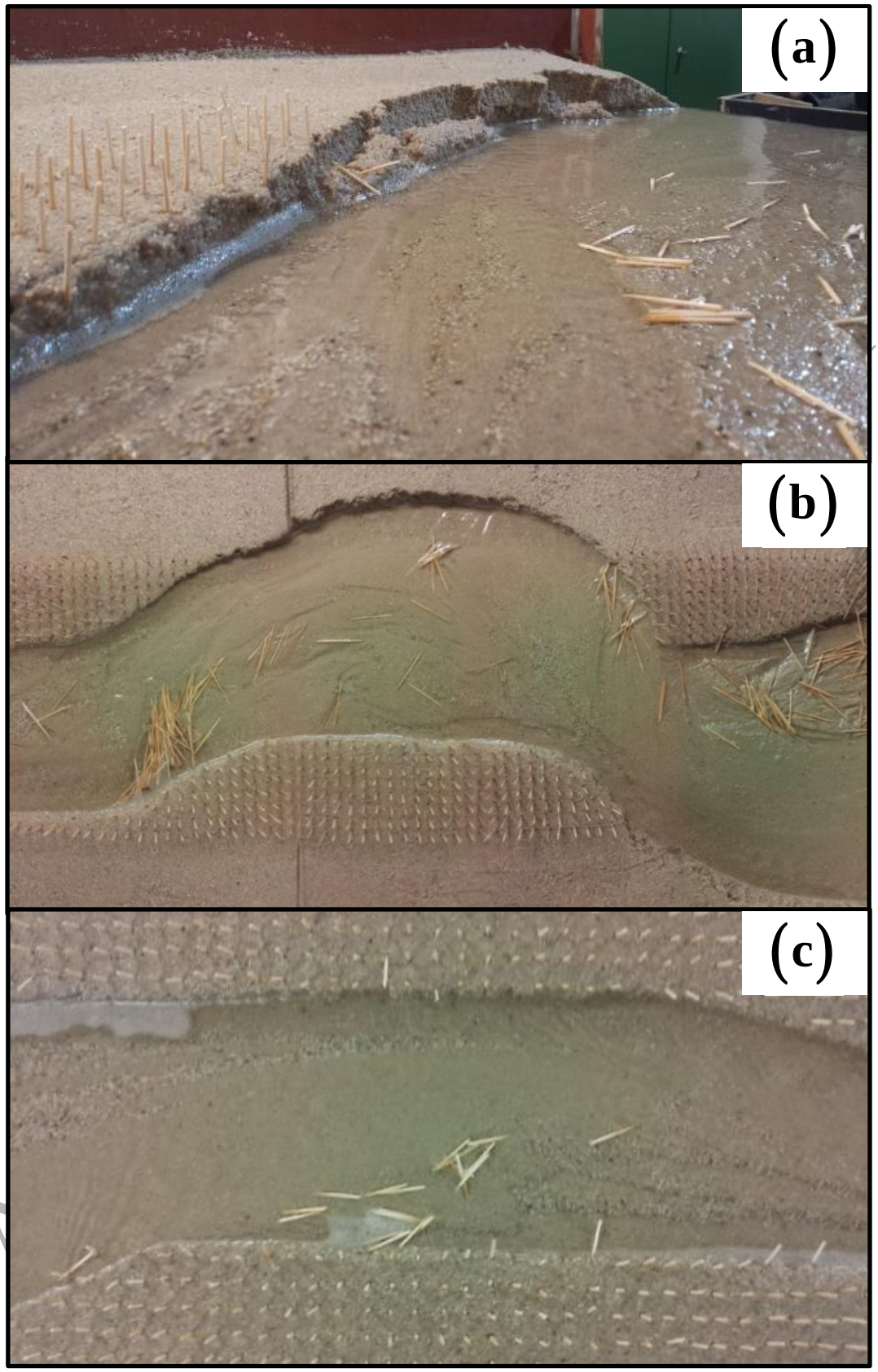

Figure 12. Processes observed in the experiments carried out in Flume No. 3: (a) bank failure (view from upstream); (b) large wood deposition (view from above), and (c) Scroll bars formation (view from above).

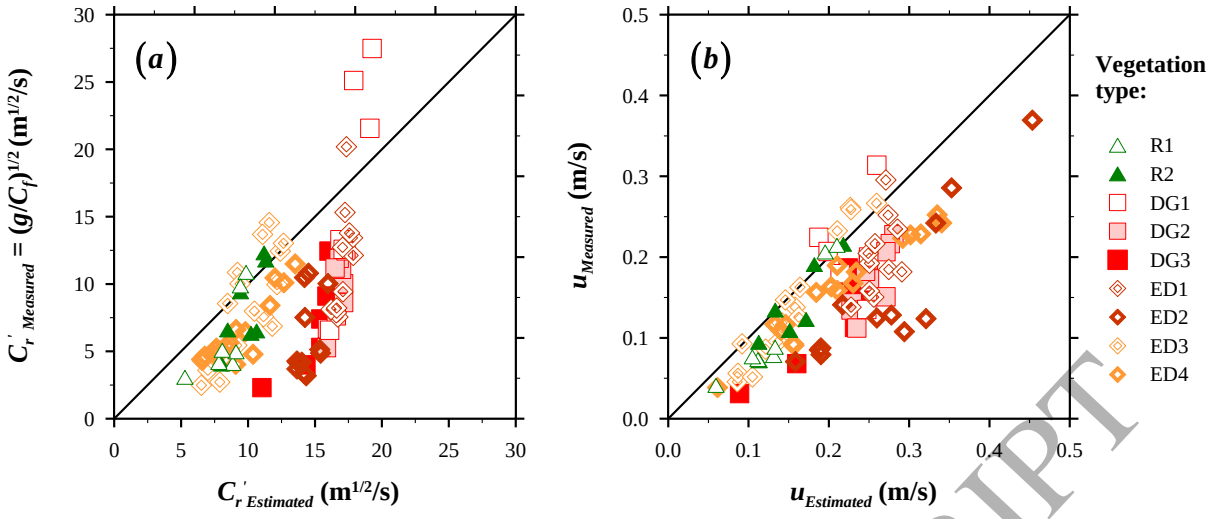

Figure 13. Measured and estimated Chézy coefficient and mean flow velocity for real and artificial plants at submerged conditions: (a) Chézy coefficient, and (b) mean flow velocity. Vegetation properties are listed in Table 1.

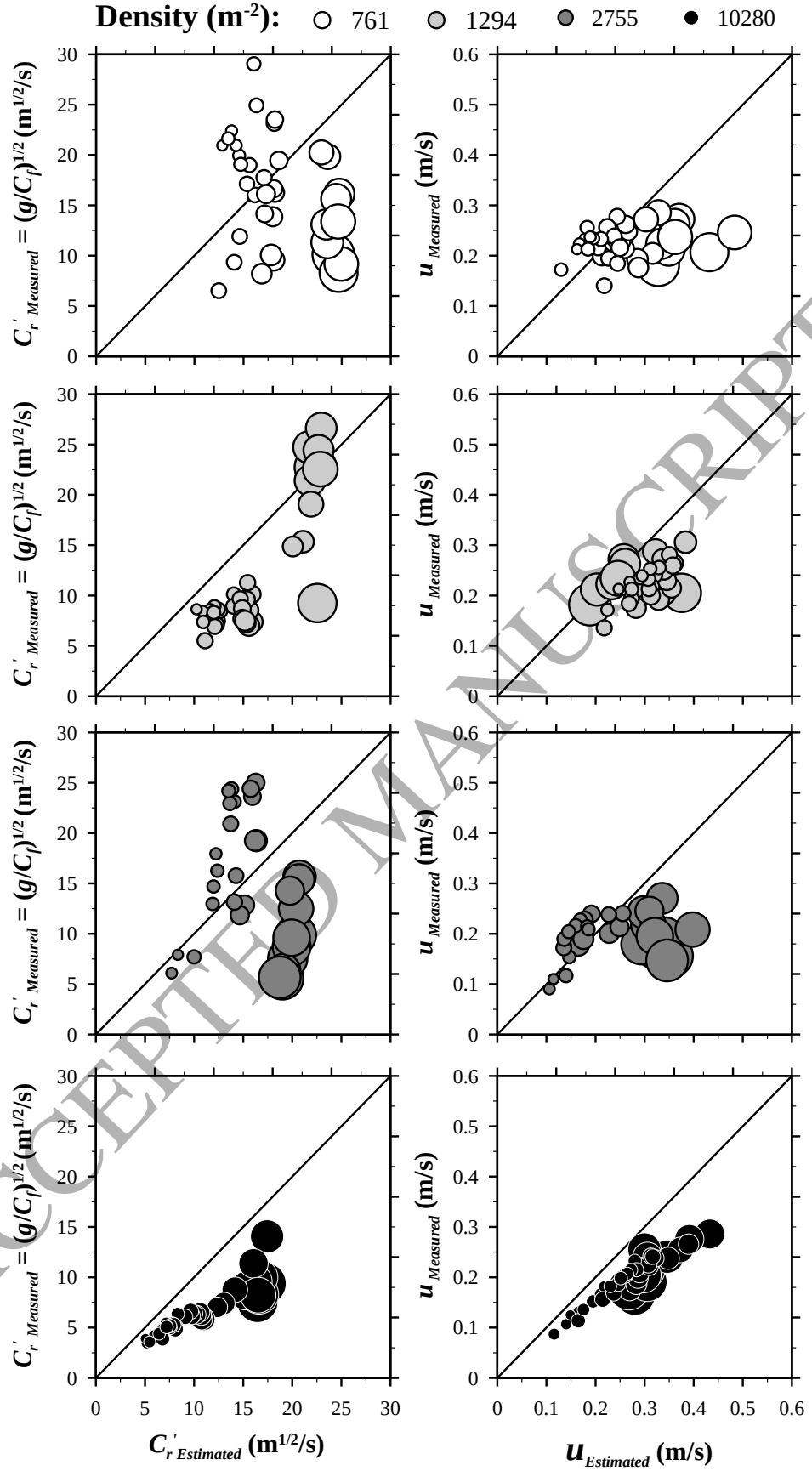

Figure 14. Measured and estimated Chézy coefficient and mean flow velocity for submerged rigid cylinders with different densities. Left panels: Chézy coefficient; right panels: mean flow velocity. Larger marker sizes indicate larger submergence ratios.

Table 1. Vegetation arrays considered in the experiments in Flume No. 1

Test[(a)]	h_v (m)	m (m^{-2})	D (m)	a (m^{-1})
W1	0.025	761	0.0020	1.5
W2	0.025	1294	0.0020	2.6
W3	0.025	2755	0.0020	5.5
W4	0.025	10280	0.0020	20.6
W5	0.050	761	0.0020	1.5
W6	0.050	1294	0.0020	2.6
W7	0.050	2755	0.0020	5.5
W8	0.050	10280	0.0020	20.6
W9	0.075	761	0.0020	1.5
W10	0.075	1294	0.0020	2.6
W11	0.075	2755	0.0020	5.5
W12	0.075	10280	0.0020	20.6
DG1	0.025	208	0.0100	2.1
DG2	0.025	656	0.0100	6.6
DG3	0.025	1296	0.0100	13.0
ED1	0.025	761	0.0088	6.7
ED2	0.025	2755	0.0088	24.2
ED3	0.050	761	0.0097	7.4
ED4	0.050	2755	0.0097	26.7
R1	0.060	761	0.0150	11.4
R2	0.060	2755	0.0150	41.3

[(a)] W: Rigid (Wooden) sticks; DG: Artificial Grass; ED: Artificial with Leaves (*Egeria densa*); R: Real (*Peperomia rotundifolia*). See Figs. 2 and 3 for graphical description.

Table 2. Vegetation arrays considered in the experiments in Flume No. 2 (for the spatial distribution see Fig. 5).

Test ID	s_1 (m)	s_2 (m)	Vegetation pattern	m (m^{-2})	a (m^{-1})
W-NV	-	-	-	-	-
W-V1	0.02	0.02	Parallel	2500	5
W-V2	0.01	0.02	Staggered	2500	5
W-V3	0.01	0.02	Parallel	5000	10
W-V4	0.02	0.01	Parallel	5000	10
W-V5	0.01	0.01	Staggered	5000	10
W-V6	0.01	0.01	Staggered	10000	20

Table 3. Vegetation arrays considered in the experiments in Flume No. 3 (for the spatial distribution see Fig. 5 and 6).

Test ID	s_1 (m)	s_2 (m)	H_1 (m)	H_2 (m)	m (m^{-2})	a (m^{-1})
P-NV	-	-	-	-	-	-
P-V1	0.04	0.02	0.08	0.06	1250	2.5
P-V2	0.04	0.02	0.08	0.01	1250	2.5
P-V3	0.04	0.02	0.04	0.01	1250	2.5
P-V4	0.02	0.02	0.08	0.06	2500	5.0

Table 4. Characteristics of vegetation adopted by: Baptist and de Jong [101] (1); Facchini et al. [105] (2); Montes Arboleda et al. [106] (3).

Vegetation type	Plant height h_v (m)	Stem diameter D (m)	Density m (m^{-2})	Canopy density $a = mD$ (m^{-1})	C_D (-)	Product $a \times C_D$ (m^{-1})
Production forest (1)	10	0.042	2	0.0840	1.0	0.0840
Close floodplain forest (1)	10	0.042	1.2	0.0504	1.0	0.0504
Open floodplain forest (1)	10	0.042	0.4	0.0168	1.0	0.0168
Close shrub (1)	5	0.010	10.2	0.1020	1.0	0.1020
Open shrub (1)	5	0.010	3.4	0.0340	1.0	0.0340
Herbaceous vegetation (1)	0.5	0.005	400	2	1.0	2
Floodplain grassland (1)	0.2	0.003	3,000	9	1.0	9
Production grassland (1)	0.1	0.003	4,000	12	1.0	12
Pioneer vegetation (1)	0.1	0.003	50	0.1500	1.0	0.1500
Pioneer vegetation (2)	0.15	0.003	50	0.150	1.8	0.270
Production grassland (2)	0.06	0.003	15,000	45	1.8	81
Natural grassland (2)	0.10	0.003	4,000	12	1.8	21.6
Herbaceous vegetation (2)	0.20	0.003	5,000	15	1.8	27
Dry herbac. vegetation(2)	0.56	0.005	46	0.230	1.8	0.414
Shrubs (2)	6	0.034	3.8	0.130	1.5	0.195
Softwood forest (2)	10	0.140	0.2	0.028	1.5	0.042
Natural grassland (3)	0.1	0.003	4,000	12	1.8	21.6
Reed (3)	2.5	0.0046	80	0.368	1.8	0.660
Softwood forest (3)	10	0.14	0.2	0.028	1.5	0.042